

Stochastic Decision Horizons for Constrained Reinforcement Learning

Nikola Milosevic^{1,2} Leonard Franz^{3,4} Daniel Haeufle^{3,4} Georg Martius^{4,5} Nico Scherf^{†,1,2} Pavel Kolev^{†,4}

Abstract

Constrained Markov decision processes (CMDPs) provide a principled model for handling constraints, such as safety and other auxiliary objectives, in reinforcement learning. The common approach of using additive-cost constraints and dual variables often hinders off-policy scalability. We propose a Control as Inference formulation based on *stochastic decision horizons*, where constraint violations attenuate reward contributions and shorten the effective planning horizon via state-action-dependent continuation. This yields survival-weighted objectives that remain replay-compatible for off-policy actor-critic learning. We propose two violation semantics, absorbing and virtual termination, that share the same survival-weighted return but result in distinct optimization structures that lead to SAC/MPO-style policy improvement. Experiments demonstrate improved sample efficiency and favorable return-violation trade-offs on standard benchmarks. Moreover, MPO with virtual termination (VT-MPO) scales effectively to our high-dimensional musculoskeletal Hyfydy setup.¹

1. Introduction

Reinforcement learning (RL) has achieved impressive results in sequential decision making and control, yet learning safe and robust behavior efficiently remains challenging in real-world systems. Practical control problems often require optimizing performance while respecting constraints such as physical limits or avoiding hazardous contacts and irreversible failures. These requirements naturally give rise to

[†]Equal supervision ¹Max Planck Institute for Human Cognitive and Brain Sciences, Leipzig ²Center for Scalable Data Analytics and Artificial Intelligence (ScalDS.AI), Dresden/Leipzig ³Hertie Institute for Clinical Brain Research & Center for Integrative Neuroscience ⁴University of Tübingen ⁵Max Planck Institute for Intelligent Systems, Tübingen. Correspondence to: Nikola Milosevic <nmilosevic@cbs.mpg.de>.

Preprint. February 5, 2026.

¹Project website with videos: <https://tinyurl.com/sdh-crl>

trade-offs between hierarchically organized objectives.

A common formalism for such problems is the constrained Markov decision process (CMDP) (Altman, 1999), which augments reward maximization with constraints on expected cumulative costs, often enforced via Lagrangian dual variables. While CMDPs provide a clean abstraction, they introduce a persistent tension between principled constraint handling and effective off-policy learning. This tension is exacerbated in methods inspired by constrained optimization (Achiam et al., 2017b; Ray et al., 2019; Stooke et al., 2020), which typically rely on coupled primal-dual updates and are either designed for on-policy methods or introduce non-stationary targets for off-policy critic learning.

At the same time, strict constraint handling during learning may not be necessary. In natural learning systems, unsuccessful or undesired behavior often provides critical information about system dynamics and control limits. From an RL perspective, this raises a central question: *how can an agent reuse undesired experience off-policy without allowing such events to dominate long-horizon credit assignment?*

Motivated by this question, we study a relaxed, termination-style alternative to additive-cost CMDPs. Rather than enforcing explicit violation budgets via dual variables, constraint violations attenuate the agent’s effective planning horizon, yielding an explicit trade-off between problem relaxation and scalable off-policy learning. Termination-style constraint relaxations have appeared in prior work (Sun et al., 2022; Chane-Sane et al., 2024), but they are typically paired with on-policy optimization and can be sample-inefficient. We derive a *novel* probabilistic objective that turns stochastic termination signals into replay-compatible off-policy actor-critic updates. Our goal is not to recover general CMDP guarantees, but to obtain a stable, replay-compatible framework that yields useful trade-offs between conflicting objectives while scaling to challenging, realistic high-dimensional domains (e.g., musculoskeletal control).

Stochastic decision horizons. We introduce *stochastic decision horizons* (SDH) within the Control as Inference (CaI) framework (Toussaint et al., 2006; Rawlik et al., 2012; Levine, 2018). Each state-action pair is assigned a continuation probability that models stage-wise feasibility. Constraint violating events reduce the probability that a trajec-

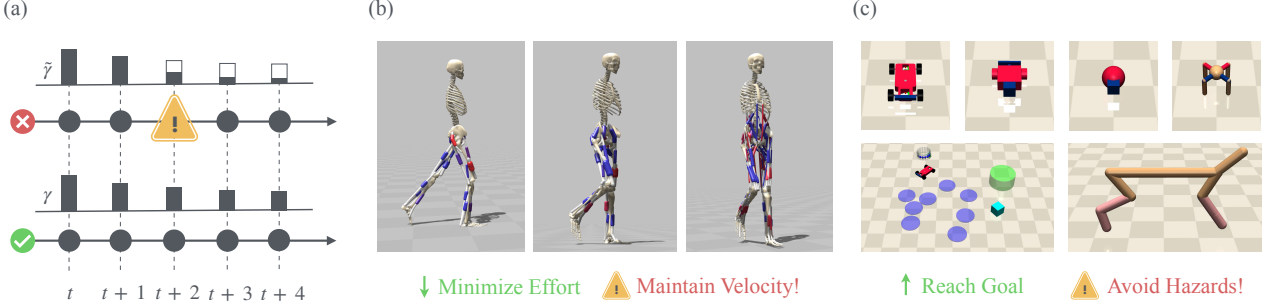


Figure 1. Overview of stochastic decision horizons (SDH) and evaluation domains. (a) SDH modulates the planning horizon via continuation probabilities (α), inducing variable discounting $\tilde{\gamma} = \gamma\alpha$ and survival-weighted returns $\tilde{r} = \alpha r$. (b) Hyfydy humanoid locomotion tasks, where low-effort gait optimization is constrained by a target walking speed. (c) Safety Gymnasium environments, which combine goal-reaching rewards with standardized hazard costs.

tory continues, while feasible regions preserve the nominal horizon. This induces a *survival-weighted* control objective that is equivalent (in value and optimal policy) to control in an MDP with state-action-dependent discounting and a shaped reward. Crucially, constraints enter entirely through modified Bellman targets in the critic, while standard off-policy policy-update machinery, including entropy regularization and replay, remains intact.

Throughout the paper, SDH denotes the general modeling device of a state-action-dependent continuation probability $\alpha(s, a) \in [0, 1]$, which shortens the effective planning horizon in infeasible regions by attenuating immediate reward contributions and discounting future terms more aggressively. We formalize this via a survival-shaped reward and state-action-dependent discount (Sec. 4). Prior methods (Sun et al., 2022; Chane-Sane et al., 2024) correspond to particular *design choices* for α driven by constraint signals (often paired with on-policy optimization). We recover those as a special cases of SDH (App. D). While distinct from general CMDPs, SDH admits a principled interpretation as an approximation to constrained control (App. D.3). This provides a justification for using SDH to approximate CMDP solutions while retaining replay compatibility and stable return-violation trade-offs.

A key modeling choice is how to interpret continuation after a violation. Under the **absorbing state** (AS) semantics, a violation induces true termination: the episode ends and no further actions are taken. Under **virtual termination** (VT), the agent continues to act, but any rewards accumulated after a violation are excluded from the optimality likelihood. Although AS and VT yield the same survival-weighted return, they differ in how regularization interacts with the control objective. In particular, AS preserves a standard *soft Bellman* recursion, which directly motivates a Soft Actor-Critic (SAC)-style algorithm (Haarnoja et al., 2018); we refer to this variant as AS-SAC. In contrast, VT is naturally compatible with KL-budgeted policy improvement, giving rise

to a corresponding modification of Maximum-a-Posteriori Policy Optimization (MPO) (Abdolmaleki et al., 2018b), which we denote VT-MPO.

We evaluate the proposed methods on Safety Gymnasium (Ji et al., 2023) and high-fidelity humanoid locomotion in Hyfydy (Geijtenbeek, 2021). Across domains, SDH-based methods improve sample efficiency and return-violation trade-offs compared to CMDP baselines. We further show robust scaling to realistic high-dimensional musculoskeletal control without Lagrange multipliers.

Contributions.

- **ELBOs for stochastic decision horizons (AS/VT).** We derive two evidence lower bound (ELBO) objectives (AS and VT) and show they share the same survival return, inducing shaped reward and state-action-dependent discounting in the critic.
- **Off-policy algorithms with SAC/MPO-style updates.** We instantiate VT with MPO-style KL-budgeted policy improvement (VT-MPO), and AS with SAC-style soft Bellman updates (AS-SAC), where continuation probabilities shape critic targets (via survival-weighted reward/discount) while replay compatibility is preserved. Under AS we also design a two-critic decomposition that enables principled off-policy temperature learning.
- **Empirical trade-offs without dual schemes.** On Safety Gymnasium and Hyfydy, our methods improve sample efficiency and strengthen return-violation trade-offs over strong CMDP baselines. In realistic high-dimensional Hyfydy musculoskeletal control models, VT-MPO scales robustly and improves over the state-of-the-art EWA baseline in our minimal setup (Schumacher et al., 2025), avoiding Lagrange multipliers.

2. Related Work

On-policy methods for constrained RL. Most constrained RL algorithms combine policy gradients with constrained optimization techniques, including primal-dual methods (Ray et al., 2019; Stooke et al., 2020), trust-region approaches (Achiam et al., 2017b; Yang et al., 2020; Zhang et al., 2020; Milosevic et al., 2025), and (barrier) penalty methods (Liu et al., 2020; Zhang et al., 2022; 2025; Dey et al., 2024; Usmanova et al., 2024). While these methods offer strong theoretical guarantees, they are typically on-policy, limiting their scalability in modern continuous-control settings.

Off-policy methods for constrained RL. Off-policy constrained RL remains comparatively underexplored. Recent work in safe offline RL includes advantage-weighted regression (Koirala et al., 2024) and diffusion-based policies (Zheng et al., 2024). Other approaches can, in principle, be combined with off-policy learning: state-augmentation methods target almost-sure safety (Sootla et al., 2022), epigraph-based stabilize-avoid objectives can be optimized with deep RL (So & Fan, 2023), and model-based methods remain a common choice for safe exploration (Berkenkamp et al., 2017; As et al., 2025), despite their own limitations, such as compounding model errors.

Constraint-based problem formulations. Constrained Markov decision processes (CMDPs) formalize reward maximization under expected cumulative cost constraints (Altman, 1999), including chance-constrained variants (Charnes & Cooper, 1959). They have been widely used to model compositional objectives (Roy et al., 2022), quality-diversity trade-offs (Zahavy et al., 2023), safe reinforcement learning (Ray et al., 2019), and safe exploration in RL (As et al., 2025). Related formulations include risk-sensitive objectives that control tail events or return distributions (Chow et al., 2018; Dabney et al., 2018). A complementary line of work adopts *termination-style relaxations*, where rewards are truncated or down-weighted after constraint violations (Sun et al., 2022; Chane-Sane et al., 2024). Our approach follows this perspective, but derives the objective from first principles using Control as Inference (Toussaint et al., 2006; Rawlik et al., 2012; Levine, 2018).

Control as Inference. Control as Inference (CaI) casts entropy-regularized RL as variational inference (Levine, 2018). Soft Actor-Critic (SAC) (Haarnoja et al., 2018) arises as a special case, while relative-entropy policy iteration methods such as Maximum-a-posteriori Policy Optimization (MPO) (Abdolmaleki et al., 2018b;a) can be interpreted as coordinate ascent on the CaI objective. MPO and related methods have been extended to multi-objective and distributional settings (Rojers et al., 2013; Abdolmaleki et al.,

2020; Huang et al., 2022), and have proven effective for learning complex robotic skills (Haarnoja et al., 2024).

Embodied exploration and musculoskeletal control. Musculoskeletal control involves large, over-actuated action spaces and challenging exploration. DEP-RL (Schumacher et al., 2023) improves sample efficiency by intermittently switching to an embodied exploration controller while training MPO off-policy from replay. Complementary to exploration, Effort Weight Adaptation (EWA) (Schumacher et al., 2025) uses a heuristic adaptive dual scheme that tunes an effort penalty to meet target-velocity requirements. Our work is orthogonal: SDH is a replay-compatible, termination-style CaI formulation that shapes the return via state-action-dependent continuation, avoiding Lagrange multipliers and adaptive dual schemes.

3. Background

We briefly review Control as Inference (CaI) and entropy-regularized reinforcement learning, emphasizing aspects that are essential for incorporating stochastic decision horizons and constraints. Throughout, we consider infinite-horizon Markov decision processes (MDPs) with state space $s \in \mathcal{S}$, action space $a \in \mathcal{A}$, transition kernel $P(s' | s, a)$, reward function $r(s, a) \geq 0$, and discount factor $\gamma \in (0, 1)$. A stochastic policy $\pi(a | s)$ induces a trajectory distribution $\tau = (s_0, a_0, s_1, \dots)$. All expectations are taken with respect to this distribution unless stated otherwise. Finally, we assume that constraints are mediated through a constraint violation signal $c_i(s, a) \geq 0$ for each constraint i .

Control as Inference. Regularized RL augments expected return with a convex per-state policy regularizer, unifying entropy bonuses and KL penalties to a reference policy π' within a common framework (Geist et al., 2019). Control as Inference (CaI) provides a probabilistic interpretation of this objective by casting control as approximate inference in a graphical model with optimality variables (Toussaint et al., 2006; Rawlik et al., 2012; Levine, 2018). In its standard form, CaI yields the following variational objective

$$\mathcal{J}(\pi, \pi') = \mathbb{E}_{\tau \sim \pi} \left[\sum_{t \geq 0} \gamma^t (r(s_t, a_t) - \kappa \text{KL}_t) \right], \quad (1)$$

where $\kappa > 0$ controls the strength of regularization and $\text{KL}_t := \text{KL}(\pi(\cdot | s_t) \| \pi'(\cdot | s_t))$ is a per-step divergence.

When the reference policy π' is chosen to be uniform over the action space, the KL term reduces (up to an additive constant) to the negative entropy of the policy. This recovers the familiar entropy-regularized RL objective underlying algorithms such as SAC. Crucially, CaI clarifies that entropy regularization is not an ad hoc modification, but arises from a principled variational objective.

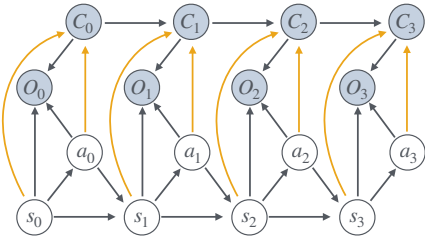


Figure 2. Control as Inference (CaI) casts optimal control as variational inference in a probabilistic graphical model (PGM). The figure shows an infinite-horizon CaI-PGM, where a Bernoulli variable (C_t) encodes continuation depending on state-action events.

Soft Bellman operators. For objectives of the form (1), policy evaluation leads to a *soft* Bellman operator, which is a contraction under standard assumptions. Contraction enables stable off-policy actor-critic algorithms using replay buffers and target networks.

Discounting as stochastic termination. A useful interpretation of discounting is as a Bernoulli survival process. At each time step, the trajectory continues with probability γ and terminates otherwise. This view suggests a natural generalization in which the continuation probability depends on the current state and action.

4. Control as Inference with Stochastic Decision Horizons

We incorporate constraints into CaI by introducing a *continuation probability* $\alpha(s, a) \in [0, 1]$ that depends on constraint violation. Intuitively, constraint-violating state-action pairs shorten the effective decision horizon by attenuating reward contributions and discounting future terms more aggressively as the region becomes more infeasible.

SDH as the general continuation model. We emphasize that SDH refers to *any* continuation model $\alpha(s, a)$, independent of a particular constraint-to-termination mapping. This perspective cleanly subsumes prior termination-style relaxations such as CaT (Chane-Sane et al., 2024) as special cases (App. D), and it yields *closed-form* CaI objectives under two continuation semantics, detailed below, that naturally motivate SAC/MPO-style updates.

Building on the stochastic-termination view of discounting (Sec. 3), we generalize continuation from a constant rate to a state-action-dependent survival model. Constraints enter through a binary continuation variable $C_t \sim \text{Bernoulli}(\alpha(s_t, a_t))$, where $\alpha : \mathcal{S} \times \mathcal{A} \rightarrow [0, 1]$ is a continuation probability from a violation signal via $\alpha(s, a) = f(c(s, a))$ for some $f : \mathbb{R}_+ \rightarrow [0, 1]$ (cf. Sec. 6.1).

Two continuation models. A subtle but important point is that “continuation” has two semantics. When $C_t = 0$, either (i) the *decision process* ends in an **absorbing state** (AS), so no further actions are taken, or (ii) only *reward collection* ends while actions continue, which we call **virtual termination** (VT). Both semantics induce the same survival-weighted return (infeasibility truncates which rewards contribute), but they differ in how regularization accumulates: under AS, post-failure *decisions* do not exist and therefore incur no KL/entropy terms, whereas under VT, post-failure actions are still taken and remain regularized.

Let the prior policy be π' and the candidate policy be π . For notational convenience, define the shaped reward $\tilde{r}(s, a) := \alpha(s, a)r(s, a)$ and effective discount $\tilde{\gamma}(s, a) := \gamma \alpha(s, a)$. *Under our survival-to-reward CaI construction* (Sec. C), these shaped terms appear directly in the ELBO, yielding the closed-form AS/VT objectives in Thm. C.1.

Proposition 4.1 (ELBO objectives for AS/VT). *Define the survival-return and survival-discount weights (with $u_0 = 1$)*

$$J_{\text{surv}}(\pi) := \mathbb{E}_{\tau \sim \pi} \left[\sum_{t \geq 0} u_t \tilde{r}(s_t, a_t) \right], \quad u_t := \prod_{k=0}^{t-1} \tilde{\gamma}(s_k, a_k).$$

Then the two semantics induce distinct variational objectives:

$$\mathcal{J}_{\text{AS}}(\pi, \pi') = J_{\text{surv}}(\pi) - \kappa \mathbb{E}_{\tau \sim \pi} \left[\sum_{t \geq 0} u_t \text{KL}_t \right], \quad (2)$$

$$\mathcal{J}_{\text{VT}}(\pi, \pi') = J_{\text{surv}}(\pi) - \kappa \mathbb{E}_{\tau \sim \pi} \left[\sum_{t \geq 0} \gamma^t \text{KL}_t \right]. \quad (3)$$

The two variational objectives in Prop. 4.1 share the same survival return but differ in how KL regularization accumulates. Our approach replaces explicit constraint violation budgets by hazard-aware horizon shaping and optimize the resulting unconstrained survival objective with KL-regularized policy improvement.

We defer the full ELBO derivation to Thm. C.1. For both AS and VT, policy evaluation reduces to a Bellman-style recursion with a *state-action-dependent discount* (Sutton et al., 1998): infeasible choices shorten the effective horizon and suppress future contributions. Crucially for our setting, the resulting variable-discount Bellman operator remains a contraction with modulus $\sup_{s, a} \tilde{\gamma}(s, a) \leq \gamma$ (Lem. C.6), thus it admits a unique fixed point and supports stable off-policy backups with replay buffer.

Relation to constrained frameworks. SDH replaces additive constraint budgeting with *horizon shaping*: constraint violations suppress future reward contributions through the survival gate induced by α . This relaxation improves replay compatibility and stabilizes long-horizon credit assignment under off-policy reuse. Although SDH is not equivalent

to additive-cost CMDPs without further assumptions, it admits principled connections to constrained and chance-constrained formulations. In particular, App. D.3 derives a finite-horizon, certificate-style chance bound for exponential continuation, making precise how SDH induces probabilistic control over violations. These results clarify when and why SDH serves as a meaningful surrogate for constrained control, even without explicit feasibility guarantees.

5. Algorithmic Framework

We next show that the AS semantics induce a soft Bellman objective that is directly compatible with SAC, whereas the VT semantics match MPO’s policy-improvement view, by recovering its partial E-step under per-state KL constraints.

5.1. Direct solution of CaI-AS

The AS objective in Prop. 4.1 induces a soft Bellman operator under $(\tilde{r}, \tilde{\gamma})$. Thus CaI-AS reduces to entropy-regularized control with state-action-dependent discounting: standard off-policy actor-critic machinery applies, with constraints entering only through the critic backup via $(\tilde{r}, \tilde{\gamma})$. With a uniform prior π' , the KL term becomes an entropy bonus, yielding a SAC-style instantiation (AS-SAC).

A subtle implication of AS is how the reference policy enters the objective. Even for a normalized uniform prior π' , the $-\log \pi'$ component in the KL term is constant per step but *not* globally constant under AS, as it accumulates with survival weights u_t , yielding a term proportional to

$$Z(\pi) := \mathbb{E}_{\tau \sim \pi} \left[\sum_{t \geq 0} u_t \right]. \quad (4)$$

Corollary G.1 shows that, under AS with a normalized uniform prior, CaI-AS is SAC-like on the survival-shaped MDP but includes an additional feasibility-weighted living cost: a constant per-decision penalty. Since decisions are only accumulated while the process survives, its expected total contribution scales as $\kappa Z(\pi)$. Counter-example G.3 further shows that, unlike standard SAC, dropping this term can change the optimizer. Nevertheless, SAC-style updates remain applicable by our two-critic decomposition detailed below.

Off-policy temperature (κ) learning under AS. Since the living-cost term scales with the policy-dependent decision mass $Z(\pi)$, constants that are ignorable in standard SAC become π -dependent, so naive temperature adaptation is generally inconsistent with the exact CaI-AS objective. We address this with a novel two-critic decomposition that separates reward and information terms under the same survival discounting, yielding TD targets independent of κ and enabling a principled off-policy dual update (App. G).

5.2. Coordinate ascent with VT-MPO

Under VT, post-violation steps can still incur information cost, but only with the base discount γ^t (Prop. 4.1). Since the reward and KL terms are weighted by different discount sequences (u_t vs. γ^t), VT does not reduce to a single soft Bellman objective in the original MDP, and therefore does not admit SAC-style regularized policy evaluation.

Instead of SAC, we apply MPO to solve VT. In this setting, MPO can be viewed as optimizing a tractable coordinate-ascent surrogate that uses the unregularized survival critic for the improvement step. Our reasoning is that MPO maximizes an ELBO objective by first performing a partial E step, which evaluates the action-value function on the *unregularized* return. Applied to VT, this means MPO’s action-value function becomes the unregularized survival critic Q_{surv}^π , which admits a standard Bellman operator. It is obtained by evaluating π under the survival-shaped dynamics in (3).

As in MPO, Q_{surv} can be learned off-policy with replay and target networks. The only modification is that TD targets use the survival-shaped $(\tilde{r}, \tilde{\gamma})$. We employ TD(n) in practice (Sec. 6). Given Q_{surv}^k at iteration k , the MPO E/M updates are unchanged. The E-step forms a KL-constrained improvement distribution using Q_{surv}^k as the score, and the M-step fits the parametric actor to that distribution (App. F).

5.3. Algorithmic consequences

The two continuation semantics lead to qualitatively different optimization structures. Under AS semantics, a violation ends the decision process, so both reward and KL regularization are accrued only while the agent remains “alive”. This collapses the problem to a KL/entropy-regularized control objective with state-action-dependent discount $\tilde{\gamma}(s, a) \leq \gamma$, and therefore admits standard soft Bellman evaluation and SAC-style updates with minimal changes.

Under VT semantics, actions are still taken after violations and the KL cost remains discounted by γ^t , which breaks the collapse and naturally aligns with MPO-style policy improvement driven by the survival-shaped critic. In practice, AS is more faithful when violations truly terminate the episode, whereas VT is useful when the system continues after failure and we want to reuse post-violation experience without letting it dominate long-horizon credit assignment.

In practice, both model a decision process but with different assumptions about the dynamics. Similar to standard discounting, they don’t have to lead to true termination in environment interactions, but only influence the objective.

6. Implementation Details

We describe the minimal deviations from standard off-policy actor-critic algorithms (SAC/MPO). In all variants, SDH

affects learning *only* through critic targets by computing a continuation probability $\alpha_t = \alpha(s_t, a_t)$ from violation signals and shaping targets via $\tilde{r}_t = \alpha_t r_t$ and $\tilde{\gamma}_t = \gamma \alpha_t$. Under AS with a normalized uniform prior, the objective includes an additional constant penalty per decision (App. G); in continuous control, we treat this term as an optional stabilization and also report an ablation in which it is omitted.

Virtual termination and `done` handling. While AS and VT *model* the decision process with terminations, the environments are not really reset on violations, and episodes end only when the simulator returns `done`. At each step, constraints define $\alpha_t = \alpha(s_t, a_t) \in [0, 1]$, yielding shaped rewards $\tilde{r}_t = \alpha_t r_t$ and discount $\tilde{\gamma}_t = \gamma \alpha_t$. For true terminal transitions we disable bootstrapping by multiplying the bootstrap term by $(1 - \text{done})$. For time-limit truncations, bootstrapping is allowed via a timeout mask, following standard off-policy practice.

6.1. Continuation model

The theory only requires $\alpha(s, a) \in [0, 1]$ and interprets it as a state-action-dependent continuation probability (Sec. 4). In practice, the specific parameterization of α is a modeling choice that determines how sharply violations attenuate the effective decision horizon, which can strongly affect stability in off-policy learning. We therefore use two simple mappings that match the regimes encountered in our benchmarks: a smooth hazard model for Safety Gymnasium, and a normalized, saturating hazard for Hyfydy where constraint magnitudes are heterogeneous and can exhibit large spikes.

Exponential continuation (Safety Gymnasium). Given violation magnitudes $c_i(s, a) \geq 0$, define $\alpha_{\text{exp}}(s, a) := \exp(-\lambda \sum_{i \in I} c_i(s, a))$. This choice provides a smooth and monotone attenuation of continuation with violation magnitude, which we find to be more robust than hard indicator-style truncation in Safety Gymnasium. Prop. D.3 additionally provides an interpretation of α_{exp} as inducing a multiplicative risk-sensitive / hazard surrogate objective; while not equivalent to chance constraints in general, it motivates the exponential form as a reasonable and stable relaxation when reusing infeasible experience off-policy.

CaT-style normalized continuation (Hyfydy). To approximate stepwise feasibility in high-fidelity musculoskeletal control, we set α using an aggregated termination probability, following Constraints as Terminations (CaT) (Chane-Sane et al., 2024). Compared to Safety Gymnasium, Hyfydy violations arise from multiple physical quantities with different units and scales, so an explicit normalization and saturation mechanism is beneficial for conditioning. Given violation magnitudes $c(s, a) \geq 0$, define

$\alpha_{\text{CaT}}(s, a) := 1 - p^{\max} \text{clip}(\frac{c(s, a)}{\max(c_{\max}, \varepsilon)}, 0, 1)$. With multiple constraints, we compute per-constraint hazards and aggregate via $\alpha(s, a) = \min_i \alpha_i(s, a)$. We maintain the scale c_{\max} using a batch moving average, which makes α less sensitive to raw cost scaling and improves robustness under nonstationary exploration.

6.2. Critic learning

Critic learning in CaI-AS. All CaI-AS variants retain the standard SAC critic machinery (double- Q , target networks, replay); constraints enter *only* through survival shaping of the Bellman backup. For a replay transition $(s, a, r, s', d) \sim \mathcal{D}$ with terminal indicator $d \in \{0, 1\}$, define $\alpha = \alpha(s, a)$, the shaped reward $\tilde{r} = \alpha r$, and the action dependent discount $\tilde{\gamma} = (1 - d)\gamma\alpha$. Sampling $a' \sim \pi_\phi(\cdot | s')$, we form the soft next-state value $\hat{V}(s') := \min_{i \in \{1, 2\}} \bar{Q}_{\bar{\theta}_i}(s', a') - \kappa \log \pi_\phi(a' | s')$, where $\kappa > 0$ is a temperature, and regress each critic to the target $y := \tilde{r} - \kappa c_{\text{LC}} + \tilde{\gamma} \hat{V}(s')$. The AS-SAC variants share this backup and differ only in the living-cost constant c_{LC} . A detailed derivation of the living-cost term and its algorithmic consequences, including a principled off-policy κ temperature update via a two-critic decomposition with TD targets independent of κ , is given in App. G. Standard AS-SAC includes the feasibility-weighted living cost, $c_{\text{LC}} = \mathcal{H}_{\text{tgt}}$. Ablations include dropping the living cost ($c_{\text{LC}} = 0$), using naive SAC-style κ tuning, and constant α , see App. B.1.3.

Critic learning in VT-MPO. Critic learning in MPO-style algorithms is commonly implemented with multi-step bootstrapped targets. While RETRACE (Munos et al., 2016) was suggested in the original MPO formulation as an off-policy correction, simple n -step returns often provide a favorable trade-off between stability and computational efficiency in deep off-policy actor-critic implementations (Hoffman et al., 2020; Pardo, 2020; Yarats et al., 2021). Following this approach, during rollout, we maintain a rolling window and precompute the survival-shaped return $R_{t, \tilde{\gamma}}^{(n)} = \sum_{k=0}^{n-1} u_{t,k} \tilde{r}_{t+k}$ and variable discount $u_{t,k} = \prod_{j=0}^{k-1} \tilde{\gamma}_{t+j}$. Each replay entry stores $(s_t, a_t, R_{t, \tilde{\gamma}}^{(n)}, s_{t+n}, u_{t+n}, \text{done})$, where u_{t+n} is the single bootstrapping continuation factor. We regress state-action function Q onto the TD(n) target $R_{t, \tilde{\gamma}}^{(n)} + (1 - \text{done}) u_{t+n} \mathbb{E}_{a \sim \pi(\cdot | s_{t+n})} [Q_{\phi^-}(s_{t+n}, a)]$, approximating the expectation by averaging target critic values over multiple actions sampled from the actor. Since this compressed n -step format does not retain the full sequence information needed for per-step importance weighting, we do not apply sequence-based corrections (e.g., Retrace) and instead use TD(n) regression with the stored u_{t+n} . Since $\tilde{\gamma}(s, a) = \gamma \alpha(s, a)$ depends on intermediate replayed actions, TD(n) targets can be biased off-policy; we use this lightweight approximation for scalability and find it stable

empirically. See App. F for details.

7. Experiments

7.1. Experimental Setup

Our experiments aim to answer three questions: do SDH-based algorithms (i) reduce constraint violations while preserving return, (ii) improve sample efficiency in off-policy settings with distinct exploration policies, and (iii) realize useful safety and multi-objective trade-offs.

We evaluate SDH-based algorithms on (i) Safety Gymnasium (Ji et al., 2023), a standard constrained continuous-control benchmark featuring hazard-style costs, and (ii) locomotion within Scone-Hyfydy (Geijtenbeek, 2019) musculoskeletal environments. The latter provides a rigorous testbed for hierarchical multi-objective control and off-policy learning in complex, high-dimensional systems.

On Safety Gymnasium, we consider 8 environments (4 locomotion, 4 navigation) and report reward-cost sample efficiency averaged over 5 seeds. We compare against unconstrained MPO and the on-policy baselines CPO (Achiam et al., 2017a) and C-TRPO (Milosevic et al., 2025), using published hyperparameters (on-policy reference points). We share environment wrappers/preprocessing and the evaluation pipeline across methods, and match step budgets and seeds unless stated otherwise. VT-MPO and AS-SAC introduce a continuation-scale parameter, which we schedule linearly during training for all environments, see App. B.1.

On Hyfydy, we evaluate VT-MPO on three humanoid walking tasks (H0918, H1622, and H2190) using a constrained formulation: minimize effort (energy) subject to a forward velocity constraint: $v_{\text{fwd}}(s_t) \geq 1.1 \text{ m s}^{-1}$. We use this minimal objective² to isolate VT-MPO’s core algorithmic properties in high-dimensional musculoskeletal control, stable learning from off-policy replay with stochastic-switch DEP exploration (Schumacher et al., 2023) and constraint-aware improvement without Lagrange multipliers. We compare against Effort Weight Adaptation (EWA) (Schumacher et al., 2025), a state-of-the-art heuristic that adapts an effort weight to meet a velocity target and has been carefully tuned in prior work; importantly, we run EWA under the same effort-velocity constrained formulation and identical training protocol as VT-MPO (see App. B.2.2 and App. B.2.4).

7.2. Results on Safety Gymnasium

Figure 3 shows that VT-MPO achieves a favorable aggregate reward-violation trade-off among the evaluated methods under our continuation-schedule protocol. Relative

²The continuation probability $\alpha(s_t, a_t)$ is computed from the violation magnitude $c_t := [1.1 \text{ m s}^{-1} - v_{\text{fwd}}(s_t)]_+$ using the CaT-style normalized continuation in Sec. 6.1.

to unconstrained MPO, both VT-MPO and AS-SAC substantially reduce cost while preserving reward. Compared to CPO and C-TRPO, they reach similar or lower violation levels with markedly higher return and faster early learning, consistent with their off-policy updates. This trend holds across most individual environments (Fig. 5), though neither method achieves feasibility on CarButton or PointGoal. Full results tables for the main benchmark, ablations, and per-environment sample-efficiency plots are provided in App. B.1.

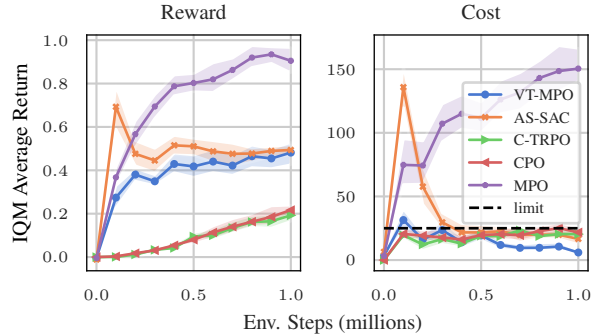


Figure 3. Aggregated sample efficiency on the Safety Gymnasium benchmark, computed using *rliable* (Agarwal et al., 2021). Curves show the interquartile mean (IQM) across environments and seeds for episodic reward (left) and cost (right) as a function of environment interactions. The reward is normalized w.r.t. unconstrained PPO at 10 million steps. Shaded regions denote 95% stratified bootstrap confidence intervals. VT-MPO and AS-SAC achieve favorable reward-violation trade-offs compared to the baselines.

Among SDH variants, AS-SAC often attains higher asymptotic return but exhibits higher variance and occasional instability. VT-MPO shows smoother learning dynamics and earlier stabilization of cost, which we attribute to MPO’s KL-regularized policy updates under variable discounting. Decreasing the continuation probability scale during training consistently improves the reward-violation trade-off (Fig. 6), supporting SDH as a continuous horizon-shaping relaxation, rather than a binary-indicator feasibility gate.

7.3. Results on Hyfydy

VT-MPO scales to high-dim musculoskeletal control and improves EWA. VT-MPO trains stably across seeds and humanoid models in our Hyfydy setup and reliably meets the target velocity while improving the effort-velocity trade-off. Across training, VT-MPO consistently improves upon the state-of-the-art EWA baseline in the energy-velocity trade-off, converging to lower-effort gaits while satisfying the imposed target-speed requirement (Fig. 4).

Stable training without dual tuning. VT-MPO meets the target-velocity constraint while improving effort, without Lagrange multipliers or adaptive dual schemes; we use a

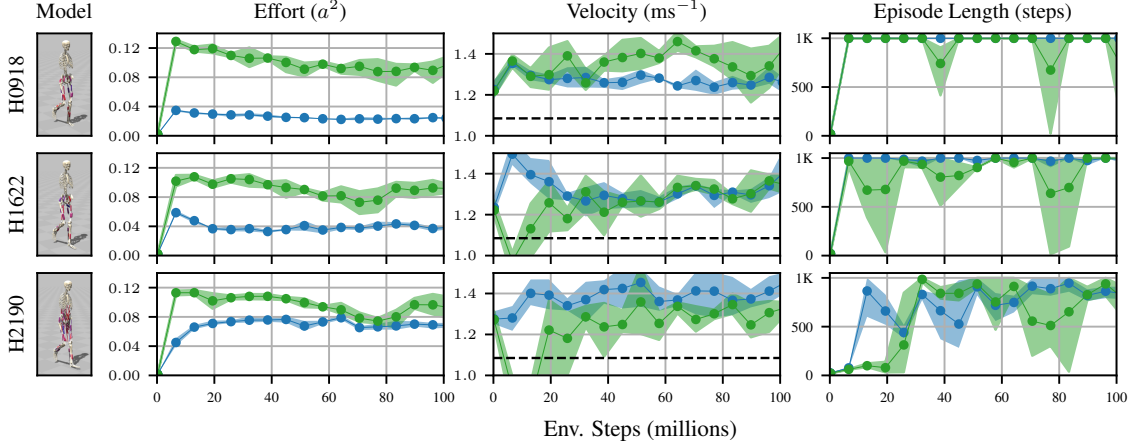


Figure 4. Hyfydy gait metrics for VT-MPO (●) and EWA (●) on H0918, H1622, and H2190 under the minimal effort-velocity constrained formulation (no extra biomechanical penalties). Curves show mean and min/max over 3 seeds; the dashed line marks the target-velocity threshold $v_{\text{fwd}}(s_t) = 1.1 \text{ m s}^{-1}$. VT-MPO converges to energy-efficient gaits while satisfying the velocity constraint.

single continuation-scale schedule shared across Hyfydy tasks. In this minimal effort-velocity constrained formulation, VT-MPO trains stably across seeds (Fig. 10).

Off-policy data utilization with DEP exploration. Abolishing the intermittent DEP exploration controller (Fig. 9) shows that VT-MPO effectively leverages highly off-policy replay data, inheriting MPO’s robustness to behavior-policy mismatch. This enables strong exploration without destabilizing the effort-velocity trade-off.

7.4. Discussion

The central empirical result is that SDH-based methods, and VT-MPO in particular, yield reliable constraint-aware solutions across qualitatively different domains without task-specific tuning or Lagrange multiplier adaptation. Most notably, in the Hyfydy musculoskeletal environments, VT-MPO consistently recovers low-effort gaits that satisfy the velocity requirement using a single continuation-scale schedule shared across tasks, producing stable solutions across seeds. This contrasts with specialized hierarchical approaches such as EWA, which rely on carefully engineered curricula and exhibit brittle training dynamics.

Addressing our three motivating questions across both benchmarks: (i) SDH-based methods reduce constraint violations without sacrificing return, (ii) remain sample-efficient in off-policy settings, and (iii) support smooth multi-objective trade-offs without Lagrange multipliers. VT-MPO is robust across tasks and seeds, while AS-SAC is more return-seeking and can reach higher reward once SDH shaping drives costs down (often below the benchmark limit), but is higher-variance when violations persist.

A limitation is that the continuation scale remains environ-

ment dependent, which would require coarse tuning to target a specific violation level. As a result, in two Safety Gymnasium tasks, neither SDH variant achieves feasibility within the training budget. We view this as an inherent trade-off of relaxing strict CMDP guarantees in exchange for replay-compatible, off-policy learning. Finally, baselines are included as reference points without exhaustive task tuning; and outcomes depend on the continuation scale/schedule, for which we report fixed settings and leave systematic sweeps/adaptive tuning to future work.

8. Conclusion

We introduced *stochastic decision horizons* (SDH), a Control as Inference formulation of termination-style constraint relaxations that replaces additive-cost budgeting with *survival-weighted* credit assignment. SDH yields critic targets with shaped reward and state-action-dependent discounting, keeping policy optimization fully compatible with off-policy replay.

We showed that two continuation semantics, absorbing state (AS) and virtual termination (VT), share the same survival-weighted return but induce distinct variational objectives and algorithmic structures, motivating SAC-style soft policy iteration under AS and MPO-style KL-budgeted improvement under VT. Across Safety Gymnasium and high-fidelity Hyfydy humanoid locomotion, SDH improves return-violation trade-offs with stable off-policy learning dynamics; notably, VT-MPO scales effectively to realistic, high-dimensional musculoskeletal models.

SDH trades CMDP-style feasibility guarantees for scalability and introduces task-dependent continuation hyperparameters. These limitations motivate future work on a unified theoretical treatment of SDH as a regularized MDP with

state-action-dependent discounting, building on the theory of regularized MDPs (Geist et al., 2019) to characterize the operator and convergence properties induced by AS vs. VT. Additional directions include adaptive or learned continuation models that target desired violation levels, *distributional SDH* critics for risk-sensitive analysis of rare violations, and extensions to offline and model-based RL.

Impact Statement

This work contributes a technical reinforcement learning objective and accompanying algorithms, evaluated in simulation, intended to improve how learning systems trade off performance and constraints. We anticipate its primary impact to be within machine learning research and benchmarking. Broader impacts, if any, would depend on downstream use in real systems; we therefore do not highlight specific societal consequences here.

Acknowledgements

Nikola Milosevic and Nico Scherf are supported by BMFTR (Federal Ministry of Research, Technology and Space) through ACONITE (16IS22065) and the Center for Scalable Data Analytics and Artificial Intelligence (ScaDS.AI) Leipzig. Georg Martius is a member of the Machine Learning Cluster of Excellence, EXC number 2064/1 – Project number 390727645. This work was supported by the ERC - 101045454 REAL-RL and the German Federal Ministry of Education and Research (BMBF): Tübingen AI Center, FKZ: 01IS18039A. The authors thank the International Max Planck Research School for Intelligent Systems (IMPRS-IS) for supporting Leonard Franz.

References

Abdolmaleki, A., Springenberg, J. T., Degrave, J., Bohez, S., Tassa, Y., Belov, D., Heess, N., and Riedmiller, M. Relative entropy regularized policy iteration. *arXiv preprint arXiv:1812.02256*, 2018a.

Abdolmaleki, A., Springenberg, J. T., Tassa, Y., Munos, R., Heess, N., and Riedmiller, M. A. Maximum a posteriori policy optimisation. In *International Conference on Learning Representations*. OpenReview.net, 2018b.

Abdolmaleki, A., Huang, S., Hasenclever, L., Neunert, M., Song, F., Zambelli, M., Martins, M., Heess, N., Hadsell, R., and Riedmiller, M. A distributional view on multi-objective policy optimization. In *International conference on machine learning*, pp. 11–22. PMLR, 2020.

Achiam, J., Held, D., Tamar, A., and Abbeel, P. **Constrained Policy Optimization**. In Precup, D. and Teh, Y. W. (eds.), *Proceedings of the 34th International Conference on Machine Learning*, volume 70 of *Proceedings of Machine Learning Research*, pp. 22–31. PMLR, 06–11 Aug 2017a.

Achiam, J., Held, D., Tamar, A., and Abbeel, P. **Constrained policy optimization**. In Precup, D. and Teh, Y. W. (eds.), *Proceedings of the 34th International Conference on Machine Learning, ICML 2017, Sydney, NSW, Australia, 6–11 August 2017*, volume 70 of *Proceedings of Machine Learning Research*, pp. 22–31. PMLR, 2017b.

Agarwal, R., Schwarzer, M., Castro, P. S., Courville, A. C., and Bellemare, M. Deep reinforcement learning at the edge of the statistical precipice. *Advances in Neural Information Processing Systems*, 34, 2021.

Altman, E. *Constrained Markov Decision Processes*. Chapman and Hall/CRC, 1999.

As, Y., Sukhija, B., Treven, L., Sferrazza, C., Coros, S., and Krause, A. **ActSafe: Active Exploration with Safety Constraints for Reinforcement Learning**. In *The Thirteenth International Conference on Learning Representations*, 2025.

Berkenkamp, F., Turchetta, M., Schoellig, A., and Krause, A. **Safe Model-based Reinforcement Learning with Stability Guarantees**. In Guyon, I., Luxburg, U. V., Bengio, S., Wallach, H., Fergus, R., Vishwanathan, S., and Garnett, R. (eds.), *Advances in Neural Information Processing Systems*, volume 30. Curran Associates, Inc., 2017.

Chane-Sane, E., Leziart, P.-A., Flayols, T., Stasse, O., Souères, P., and Mansard, N. Cat: Constraints as terminations for legged locomotion reinforcement learning. In *2024 IEEE/RSJ International Conference on Intelligent Robots and Systems (IROS)*, pp. 13303–13310. IEEE, 2024.

Charnes, A. and Cooper, W. W. Chance-constrained programming. *Management science*, 6(1):73–79, 1959.

Chow, Y., Ghavamzadeh, M., Janson, L., and Pavone, M. Risk-constrained reinforcement learning with percentile risk criteria. *Journal of Machine Learning Research*, 18(167):1–51, 2018.

Dabney, W., Rowland, M., Bellemare, M., and Munos, R. Distributional reinforcement learning with quantile regression. In *Proceedings of the AAAI conference on artificial intelligence*, volume 32, 2018.

Dey, S., Dasgupta, P., and Dey, S. P2BPO: Permeable Penalty Barrier-Based Policy Optimization for Safe RL. In *Proceedings of the AAAI Conference on Artificial Intelligence*, volume 38, pp. 21029–21036, 2024.

Geijtenbeek, T. **Scone: Open source software for predictive simulation of biological motion**. *Journal of Open Source Software*, 4(38):1421, 2019. doi: 10.21105/joss.01421.

Geijtenbeek, T. [The Hyfydy simulation software](#), 11 2021. <https://hyfydy.com>.

Geist, M., Scherrer, B., and Pietquin, O. A Theory of Regularized Markov Decision Processes. In *International Conference on Machine Learning*, pp. 2160–2169. PMLR, 2019.

Haarnoja, T., Zhou, A., Abbeel, P., and Levine, S. Soft actor-critic: Off-policy maximum entropy deep reinforcement learning with a stochastic actor. In *International conference on machine learning*, pp. 1861–1870. Pmlr, 2018.

Haarnoja, T., Moran, B., Lever, G., Huang, S. H., Tirumala, D., Humplik, J., Wulfmeier, M., Tunyasuvunakool, S., Siegel, N. Y., Hafner, R., Bloesch, M., Hartikainen, K., Byravan, A., Hasenclever, L., Tassa, Y., Sadeghi, F., Batchelor, N., Casarini, F., Saliceti, S., Game, C., Sreendara, N., Patel, K., Gwira, M., Huber, A., Hurley, N., Nori, F., Hadsell, R., and Heess, N. Learning agile soccer skills for a bipedal robot with deep reinforcement learning. *Science Robotics*, 9(89):eadi8022, 2024. doi: 10.1126/scirobotics.adi8022.

Hoffman, M. W., Shahriari, B., Aslanides, J., Barth-Maron, G., Momchev, N., Sinopalnikov, D., Stańczyk, P., Ramos, S., Raichuk, A., Vincent, D., Hussenot, L., Dadashi, R., Dulac-Arnold, G., Orsini, M., Jacq, A., Ferret, J., Vieillard, N., Ghasemipour, S. K. S., Girgin, S., Pietquin, O., Behbahani, F., Norman, T., Abdolmaleki, A., Cassirer, A., Yang, F., Baumli, K., Henderson, S., Friesen, A., Haroun, R., Novikov, A., Colmenarejo, S. G., Cabi, S., Gulcehre, C., Paine, T. L., Srinivasan, S., Cowie, A., Wang, Z., Piot, B., and de Freitas, N. Acme: A research framework for distributed reinforcement learning. *arXiv preprint arXiv:2006.00979*, 2020.

Huang, S., Abdolmaleki, A., Vezzani, G., Brakel, P., Mankowitz, D. J., Neunert, M., Bohez, S., Tassa, Y., Heess, N., Riedmiller, M., et al. A constrained multi-objective reinforcement learning framework. In *Conference on Robot Learning*, pp. 883–893. PMLR, 2022.

Ji, J., Zhang, B., Zhou, J., Pan, X., Huang, W., Sun, R., Geng, Y., Zhong, Y., Dai, J., and Yang, Y. Safety gymnasium: A unified safe reinforcement learning benchmark. In *Advances in Neural Information Processing Systems 36: Annual Conference on Neural Information Processing Systems 2023, NeurIPS 2023, New Orleans, LA, USA, December 10 - 16, 2023*, 2023.

Koirala, P., Jiang, Z., Sarkar, S., and Fleming, C. Fawac: Feasibility informed advantage weighted regression for persistent safety in offline reinforcement learning. *arXiv preprint arXiv:2412.08880*, 2024.

Levine, S. Reinforcement learning and control as probabilistic inference: Tutorial and review. *CoRR*, abs/1805.00909, 2018.

Liu, Y., Ding, J., and Liu, X. IPO: Interior-Point Policy Optimization under Constraints. *Proceedings of the AAAI Conference on Artificial Intelligence*, 34:4940–4947, 04 2020. doi: 10.1609/aaai.v34i04.5932.

Milosevic, N., Müller, J., and Scherf, N. Embedding safety into RL: A new take on trust region methods. In *International Conference on Machine Learning*. OpenReview.net, 2025.

Munos, R., Stepleton, T., Harutyunyan, A., and Bellemare, M. Safe and efficient off-policy reinforcement learning. *Advances in neural information processing systems*, 29, 2016.

Pardo, F. Tonic: A deep reinforcement learning library for fast prototyping and benchmarking. *arXiv preprint arXiv:2011.07537*, 2020.

Rawlik, K., Toussaint, M., and Vijayakumar, S. On stochastic optimal control and reinforcement learning by approximate inference. *Proceedings of Robotics: Science and Systems VIII*, 2012.

Ray, A., Achiam, J., and Amodei, D. Benchmarking Safe Exploration in Deep Reinforcement Learning. *arXiv preprint arXiv:1910.01708*, 7(1):2, 2019.

Rojers, D. M., Vamplew, P., Whiteson, S., and Dazeley, R. A survey of multi-objective sequential decision-making. *Journal of Artificial Intelligence Research*, 48:67–113, 2013. doi: 10.1613/jair.3987.

Roy, J., Girgis, R., Romoff, J., Bacon, P., and Pal, C. J. Direct behavior specification via constrained reinforcement learning. In *International Conference on Machine Learning*, Proceedings of Machine Learning Research, 2022.

Schumacher, P., Haeufle, D. F. B., Büchler, D., Schmitt, S., and Martius, G. DEP-RL: embodied exploration for reinforcement learning in overactuated and musculoskeletal systems. In *The Eleventh International Conference on Learning Representations, ICLR 2023, Kigali, Rwanda, May 1-5, 2023*. OpenReview.net, 2023.

Schumacher, P., Geijtenbeek, T., Caggiano, V., Kumar, V., Schmitt, S., Martius, G., and Haeufle, D. F. Emergence of natural and robust bipedal walking by learning from biologically plausible objectives. *iScience*, pp. 112203, March 2025. ISSN 2589-0042. doi: 10.1016/j.isci.2025.112203.

So, O. and Fan, C. Solving stabilize-avoid via epigraph form optimal control using deep reinforcement learning. In *Robotics: Science and Systems XIX, Daegu, Republic of Korea, July 10-14, 2023*, 2023.

Sootla, A., Cowen-Rivers, A. I., Jafferjee, T., Wang, Z., Mguni, D. H., Wang, J., and Ammar, H. Sauté rl: Almost surely safe reinforcement learning using state augmentation. In *International Conference on Machine Learning*, pp. 20423–20443. PMLR, 2022.

Stooke, A., Achiam, J., and Abbeel, P. Responsive safety in reinforcement learning by pid lagrangian methods. In *International Conference on Machine Learning*, pp. 9133–9143. PMLR, 2020.

Sun, H., Xu, Z., Peng, Z., Fang, M., Wang, T., Dai, B., and Zhou, B. Constrained mdps can be solved by early-termination with recurrent models. In *NeurIPS 2022 Foundation Models for Decision Making Workshop*, 2022.

Sutton, R. S., Barto, A. G., et al. *Reinforcement learning: An introduction*, volume 1. MIT press Cambridge, 1998.

Toussaint, M., Harmeling, S., and Storkey, A. Probabilistic inference for solving (po) mdps. Technical report, Technical Report EDI-INF-RR-0934, School of Informatics, University of Edinburgh, 2006.

Usmanova, I., As, Y., Kamgarpour, M., and Krause, A. Log Barriers for Safe Black-box Optimization with Application to Safe Reinforcement Learning. *Journal of Machine Learning Research*, 25(171):1–54, 2024.

Yang, T.-Y., Rosca, J., Narasimhan, K., and Ramadge, P. J. **Projection-based constrained policy optimization.** In *International Conference on Learning Representations*, 2020.

Yarats, D., Zhang, A., Kostrikov, I., Amos, B., Pineau, J., and Fergus, R. Improving sample efficiency in model-free reinforcement learning from images. In *Proceedings of the AAAI conference on artificial intelligence*, volume 35, pp. 10674–10681, 2021.

Zahavy, T., Schroecker, Y., Behbahani, F. M. P., Baumli, K., Flennerhag, S., Hou, S., and Singh, S. **Discovering policies with domino: Diversity optimization maintaining near optimality.** In *The Eleventh International Conference on Learning Representations, ICLR 2023, Kigali, Rwanda, May 1-5, 2023*. OpenReview.net, 2023.

Zhang, B., Zhang, Y., Zhu, H., Yan, S., Brox, T., and Boedecker, J. Constrained reinforcement learning with smoothed log barrier function. *Trans. Mach. Learn. Res.*, 2025.

Zhang, L., Shen, L., Yang, L., Chen, S., Wang, X., Yuan, B., and Tao, D. Penalized Proximal Policy Optimization for Safe Reinforcement Learning. In *Thirty-First International Joint Conference on Artificial Intelligence*, pp. 3719–3725, 07 2022. doi: 10.24963/ijcai.2022/517.

Zhang, Y., Vuong, Q., and Ross, K. First Order Constrained Optimization in Policy Space. *Advances in Neural Information Processing Systems*, 33:15338–15349, 2020.

Zheng, Y., Li, J., Yu, D., Yang, Y., Li, S. E., Zhan, X., and Liu, J. Safe offline reinforcement learning with feasibility-guided diffusion model. In *The Twelfth International Conference on Learning Representations, ICLR 2024, Vienna, Austria, May 7-11, 2024*. OpenReview.net, 2024.

Appendix

Table of Contents

A Algorithmic Descriptions of VT-MPO and AS-SAC	13
B Experimental Results	14
B.1 Experiments on Safety Gymnasium	14
B.2 Experiments on Hyfydy	18
C Control as Inference with Stochastic Decision Horizons	23
C.1 Control as Inference model	23
C.2 Two ELBO objectives and main result	24
C.3 Supporting lemmas	24
C.4 Proof of Thm. C.1	26
C.5 Bellman operators and contraction	27
D Relation to Constrained RL and Related Frameworks	27
D.1 Notation and setup	28
D.2 Relation to termination-style returns	28
D.3 Additive hazard and a finite-horizon chance bound for exponential continuation	29
D.4 Relation to chance constraints	30
E Algorithmic Details	30
E.1 Environment termination and <code>done</code> handling	30
E.2 Continuation models used in the experiments	30
E.3 Replay-format note for VT-MPO	31
E.4 Where to find method-specific details	31
F VT-MPO: MPO with a Survival-Shaped Critic	31
F.1 Survival critic induced by SDH	32
F.2 Policy improvement (unchanged MPO E/M steps)	32
F.3 Off-policy critic learning with variable discount	32
F.4 VT-MPO Summary	33
G Absorbing State (Real Termination): Uniform Prior Structure, AS-SAC, and Dual Temperature Updates	33
G.1 Exact CaI+AS objective under a normalized uniform prior	33
G.2 AS implies a SAC-style soft Bellman recursion under survival shaping	34
G.3 What constraint does κ optimize under AS? (Why constants matter)	35
G.4 Two-critic decomposition (targets independent of κ)	35
G.5 Off-policy TD targets and a practical dual update for κ	37
G.6 Algorithm summary (Two-Critic AS-SAC)	37

A. Algorithmic Descriptions of VT-MPO and AS-SAC

We present the VT-MPO and AS-SAC implementation faithful pseudocode in Algorithm 1 and Algorithm 2, respectively. We define parameters: cost limit b , hazard cap p^{\max} , EMA scalar $c_{\max} \leftarrow \varepsilon_c$, smoothing ρ ; violation $v_t = [c_t - c_{\lim}]_+$, stopping probability $\delta_t = p^{\max} \text{clip}(\frac{v_t}{\max(c_{\max}, \varepsilon_c)}, 0, 1)$ continuation probability $\alpha_t = 1 - \delta_t$, attenuated reward $\tilde{r}_t = \alpha_t r_t$, variable discount $\tilde{\gamma}_t = \gamma \alpha_t$.

Algorithm 1 VT-MPO (termination=Virtual; actor=MPO, critic=unregularized-survival-TD(n))

```

1: Initialize actor  $\pi_\theta$ , prior  $\pi_0$ , critic  $Q_\phi$ , target critic  $Q_{\phi^-} \leftarrow Q_\phi$ , replay buffer  $\mathcal{B}$ 
2: Initialize rolling window of length  $n$  for  $(s, a, r, c, \alpha)$ 
3: while training do
4:   Collect data (no resets on violations): run policy  $\pi_0$  in the environment; observe  $(s_t, a_t, r_t, c_t, s_{t+1}, \text{done})$ 
5:   Append  $(s_t, a_t, r_t, c_t, \alpha_t)$  to the rolling window
6:   If the rolling window has length  $n$ , compute and store in replay:
7:      $R_{t, \tilde{\gamma}}^{(n)} = \sum_{k=0}^{n-1} (\prod_{j=0}^{k-1} \gamma \alpha_{t+j}) (\alpha_{t+k} r_{t+k})$ 
8:      $u_{t,n} = \prod_{j=0}^{n-1} \gamma \alpha_{t+j}$  and bootstrap state  $s_{t+n}$ 
9:     store  $(s_t, a_t, R_{t, \tilde{\gamma}}^{(n)}, c_t, s_{t+n}, u_{t,n}, \text{done}, \log \pi(a_t | s_t))$  in  $\mathcal{B}$ 
10:  Batch-EMA scaling (periodic): sample replay costs, update  $c_{\max} \leftarrow \rho c_{\max} + (1 - \rho)[c - b]_+$ 
11:  Critic update: sample minibatch from  $\mathcal{B}$ , regress
12:     $Q_\phi(s_t, a_t) \leftarrow R_{t, \tilde{\gamma}}^{(n)} + (1 - \text{done}) u_{t,n} \mathbb{E}_{a \sim \pi(\cdot | s_{t+n})} [Q_{\phi^-}(s_{t+n}, a)]$ 
13:  Actor update (standard MPO): perform MPO E/M steps using  $Q_{\phi^-}$  as score
14:    (Implementation: MPO regression may use stacked states  $\{s_t\} \cup \{s_{t+n}\}$  for improved coverage.)
15:  Periodically update target networks  $\phi^- \leftarrow \phi$ , and optionally a slow-moving actor
16: end while

```

Algorithm 2 AS-SAC (termination=Absorbing State; actor=SAC, critic=regularized-survival-TD(0))

```

1: Init actor  $\pi_\theta$  (tanh-Gaussian), critics  $Q_{\phi_1}, Q_{\phi_2}$  and targets  $\phi_i^- \leftarrow \phi_i$ ; replay  $\mathcal{B}$  stores  $(s, a, \tilde{r}, c, s', \tilde{\gamma}, \text{done})$ 
2: Init entropy temperature  $\alpha_{\text{ent}}$  (autotune with  $\mathcal{H}_{\text{tgt}} = -\dim(\mathcal{A})$  or fixed)
3: while training do
4:   Collect: sample  $a_t$  (random if  $t < t_{\text{learn}}$ , else  $a_t \sim \pi_\theta(\cdot | s_t)$ ); step env  $\rightarrow (r_t, c_t, s_{t+1}, \text{term}, \text{trunc})$ 
5:   if truncated, set  $s_{t+1} \leftarrow s_{t+1}^{\text{final}}$ ; set  $\text{done}_t \leftarrow \text{term}$ 
6:   Compute  $(\tilde{r}_t, \tilde{\gamma}_t)$ ; store  $(s_t, a_t, \tilde{r}_t, c_t, s_{t+1}, \tilde{\gamma}_t, \text{done}_t)$  in  $\mathcal{B}$ 
7:   if  $t \geq t_{\text{learn}}$  then
8:     Critic: sample batch from  $\mathcal{B}$ ; sample  $(a', \log \pi_\theta(a' | s'))$ ;
9:     set  $\hat{Q}^-(s', a') = \min_i Q_{\phi_i^-}(s', a') - \alpha_{\text{ent}}(\log \pi_\theta(a' | s') - \mathcal{H}_{\text{tgt}})$ ; set  $y = \tilde{r} + (1 - \text{done}) \tilde{\gamma} \hat{Q}^-(s', a')$ 
10:    Update  $\phi_i$  by MSE to target  $y$  (twin critics)
11:    Periodically update
12:      Actor:  $a_\pi \sim \pi_\theta(\cdot | s)$ ;  $\max_\theta \mathbb{E}[\min_i Q_{\phi_i}(s, a_\pi) - \alpha_{\text{ent}} \log \pi_\theta(a_\pi | s)]$ 
13:      if autotune update  $\alpha_{\text{ent}}$  using loss  $-\alpha_{\text{ent}}(\log \pi_\theta(a_\pi | s) + \mathcal{H}_{\text{tgt}})$ 
14:      update target critics:  $\phi_i^- \leftarrow \tau \phi_i + (1 - \tau) \phi_i^-$ 
15:      if CaT-scaler update violation scale:  $c_{\max} \leftarrow \rho c_{\max} + (1 - \rho)[c - b]_+$ 
16:    end if
17: end while

```

B. Experimental Results

B.1. Experiments on Safety Gymnasium

B.1.1. DETAILS ON THE EXPERIMENTAL SETUP

We evaluate on a subset of 8 continuous-control tasks from Safety Gymnasium (Ji et al., 2023), which provide locomotion and navigation-style environments with standardized cost signals (e.g., hazards). The benchmark consists of 4 locomotion and 4 navigation environments. The full list can be seen in Table 1. We report average episodic returns of reward and cost per episode in the form of sample efficiency curves measured against the number of environment interactions. Each training run is repeated for 5 seeds and the sample efficiency results are aggregated across seeds for each environment. We compare against unconstrained MPO and trust-region constrained baselines CPO (Achiam et al., 2017b) and C-TRPO (Milosevic et al., 2025). Hyperparameters are taken from the respective publications, as they evaluate on the same environments. VT-MPO and AS-SAC introduce one additional hyperparameter λ that controls the mapping from constraint violations to continuation probabilities, see Section 6.1. For a fair comparison, we fix a linear schedule $\lambda \in [0, 0.9]$ between timesteps $50k$ and $500k$ for all environments.

B.1.2. MAIN RESULTS ON SAFETY GYMNASIUM

Aggregate performance. Figure 3 shows that VT-MPO achieves the most favorable aggregate return-violation trade-off. Compared to unconstrained MPO, both VT-MPO and AS-SAC substantially reduce cost while retaining competitive reward. Compared to the on-policy baselines, they reach similar or lower violation levels with substantially higher return.

Per-environment behavior. Figure 5 shows that this aggregate trend is consistent across most individual environments. VT-MPO and AS-SAC reliably suppress cost towards the end of training while improving reward rapidly early on, whereas CPO and C-TRPO are typically conservative early on and improve reward slowly, reflecting their on-policy nature. Overall, AS-SAC tends to achieve higher asymptotic return in environments where constraint satisfaction is maintained throughout training. VT-MPO, however, is more robust across tasks and seeds, which we attribute to MPO’s KL-regularized policy improvement under variable discounting. Finally, in two of the eight environments (CarButton and PointGoal), neither VT-MPO nor AS-SAC produce a feasible policy.

Single-seed dynamics. AS-SAC often achieves higher peak return once constraints are satisfied, but exhibits higher variance and occasional instability. VT-MPO shows smoother learning dynamics and earlier stabilization of cost, consistent with MPO’s trust-region policy updates and unregularized critic. Figure 6 highlights this on representative single-seed runs, especially on the Ant and HalfCheetah environments.

Effect of survival weighting. Across environments, decreasing the scale of the continuation probability α over training improves the return-violation trade-off, see Figure 6. Early in learning, higher α allows exploration of infeasible regions and reuse of infeasible transitions. Later, reduced survival weighting attenuates long-horizon credit assignment through infeasible states, guiding convergence toward feasible behavior. This supports interpreting SDH as a continuous relaxation of hard constraints rather than a binary feasibility mechanism.

B.1.3. EVALUATED AS BASELINES AND ABLATIONS

We distinguish 4 AS-SAC implementation variants: (i) **AS-SAC (full)**, which optimizes the exact objective including the penalty term implied by the normalized uniform prior, (ii) **AS-SAC (naive critic)**, which *incorrectly* removes the induced horizon regularization, (iii) **AS-SAC (κ const.)** which implements the full critic but with a constant κ , and (iv) **AS-SAC (naive tuning)**, which implements the full critic but with the standard SAC-temperature tuning, which does not require additional critic training. The “naive critic” ablation directly tests the theoretical prediction that, under AS, the uniform-prior term is not a removable constant, and the temperature tuning ablations test the merit of the living-cost-weighted tuning procedure. Table 2 demonstrates the superior performance of the naive-tuning baseline on 3 out of 8 environments. We hypothesize that this variant strikes a favorable balance between theoretical justification and gradient stability due to the constant entropy target. This is also the version we use in the main benchmark. The full version of AS-SAC is presented in Algorithm 3, where deviations from Algorithm 2 are marked in red.

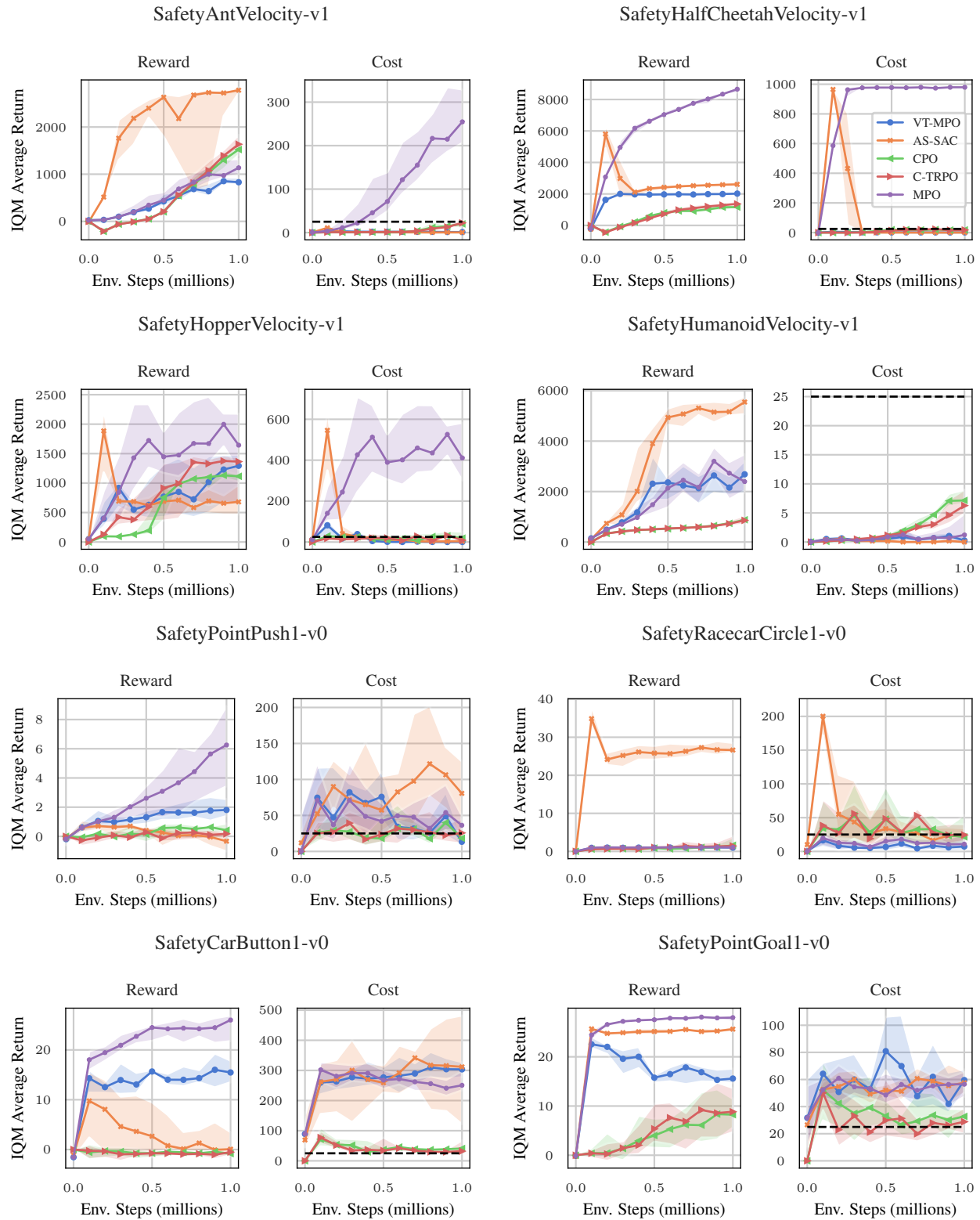


Figure 5. Results on the Safety Gymnasium benchmark for individual environments.

Table 1. Expected returns (R) and costs (C) on Safety Gymnasium after one million environment steps. The cost limit is 25.0 mean cost return (Ji et al., 2023). The algorithm with the highest inter quartile mean return (25%) among the feasible ones in an environment is marked in bold. The larger side of the confidence interval is denoted by \pm , rounded to one decimal. In CarButton and PointGoal, no algorithm yields a feasible policy in the prescribed number of environment interactions.

	AntVelocity	HalfCheetah	Humanoid	Hopper	CarButton	PointGoal	RacecarCircle	PointPush
VT-MPO (ours)	<i>R</i> 829 ± 99	2021 ± 71	2683 ± 531	1293 ± 186	15.5 ± 2.4	15.6 ± 1.7	1.0 ± -0.0	1.8 ± 0.8
	<i>C</i> 1.3 ± 0.1	1.6 ± 0.6	0.3 ± 0.7	0.2 ± 0.2	303 ± 27	59.6 ± 7.9	7.3 ± 6.8	13.4 ± 5.0
AS-SAC (ours)	<i>R</i> 2779 ± 64	2608 ± 37	5549 ± 235	681 ± 283	0.1 ± 3.4	25.6 ± 0.6	26.6 ± 1.9	-0.3 ± 0.5
	<i>C</i> 0.4 ± 0.2	0.2 ± 0.1	0.0 ± 0.0	3.5 ± 3.1	311 ± 170	57.6 ± 8.1	22.6 ± 11.6	80.7 ± 42.4
C-TRPO	<i>R</i> 1634 ± 198	1363 ± 182	857 ± 198	1364 ± 67	-0.5 ± 0.4	8.8 ± 4.9	1.4 ± 2.8	0.2 ± 0.2
	<i>C</i> 22.3 ± 9.7	17.4 ± 4.5	6.3 ± 2.7	8.4 ± 11.1	32.1 ± 35.7	28.8 ± 10.3	24.5 ± 15.9	25.7 ± 19.1
CPO	<i>R</i> 1522 ± 90	1163 ± 97	881 ± 79	1115 ± 28	-0.8 ± 0.4	8.2 ± 3.7	1.6 ± 2.1	0.4 ± 0.5
	<i>C</i> 20.0 ± 5.8	18.2 ± 9.5	7.2 ± 1.8	18.8 ± 32.2	41.0 ± 6.8	32.8 ± 5.3	21.5 ± 30.0	18.3 ± 6.9
PPO	<i>R</i> 44.6 ± 6.0	1671 ± 758	506 ± 7	491 ± 174	16.8 ± 1.2	25.2 ± 0.7	35.0 ± 2.7	0.7 ± 0.3
	<i>C</i> 1.4 ± 0.3	151 ± 266	1.3 ± 1.4	135 ± 30	333 ± 25	50.6 ± 6.1	194 ± 46	52.8 ± 36.4
MPO	<i>R</i> 1136 ± 185	8654 ± 126	2395 ± 1088	1643 ± 548	26.0 ± 0.9	28.0 ± 0.4	1.1 ± -0.0	6.3 ± 2.6
	<i>C</i> 254 ± 74	979 ± 0	1.2 ± 3.7	410 ± 172	250 ± 46	56.5 ± 9.1	10.8 ± 13.2	36.3 ± 13.3

Table 2. Expected returns (R) and costs (C) on Safety Gymnasium for the AS-SAC ablations after one million environment steps with cost limit 25.0 mean cost return (Ji et al., 2023). The algorithm with the highest inter quartile mean return (25%) among the feasible ones in an environment is marked in bold.

	Ant	HalfCheetah	Humanoid	Hopper	CarButton	PointGoal	RacecarCircle	PointPush
AS-SAC (full)	<i>R</i> 2521 ± 179	2411 ± 117	4833 ± 257	733 ± 507	-0.4 ± 0.2	25.9 ± 0.7	0.0 ± 0.2	-0.3 ± 0.3
	<i>C</i> 0.3 ± 0.3	0.3 ± 0.3	0.0 ± 0.6	0.0 ± 9.6	336 ± 182	50.2 ± 59.8	31.1 ± 52.4	74.0 ± 38.3
AS-SAC (naive critic)	<i>R</i> 1895 ± 838	2722 ± 15	5314 ± 430	794 ± 196	3.3 ± 7.2	25.6 ± 0.3	26.2 ± 1.1	-0.6 ± 0.2
	<i>C</i> 0.3 ± 0.1	0.4 ± 0.4	0.0 ± 0.4	3.1 ± 22.9	305 ± 67	64.0 ± 6.2	22.4 ± 36.9	86.9 ± 31.1
AS-SAC (κ const.)	<i>R</i> 2553 ± 18	2699 ± 17	5384 ± 343	1009 ± 50	-3.4 ± 1.5	-0.7 ± 0.3	0.1 ± 0.1	-0.6 ± 0.3
	<i>C</i> 0.5 ± 0.2	0.3 ± 0.0	0.0 ± 0.2	1.1 ± 9.2	270 ± 160	115 ± 66	0.3 ± 2.3	27.9 ± 22.0
AS-SAC (naive tuning)	<i>R</i> 2779 ± 64	2608 ± 37	5549 ± 235	681 ± 283	0.1 ± 3.4	25.6 ± 0.6	26.6 ± 1.9	-0.3 ± 0.5
	<i>C</i> 0.4 ± 0.2	0.2 ± 0.1	0.0 ± 0.0	3.5 ± 3.1	311 ± 170	57.6 ± 8.1	22.6 ± 11.6	80.7 ± 42.4

Algorithm 3 AS-SAC (full) (termination=Absorbing State; actor=SAC, critic=regularized-survival-TD(0))

```

1: Init actor  $\pi_\theta$  (tanh-Gaussian), critics  $Q_{\phi_1}, Q_{\phi_2}, Q_\nu$  and targets  $\phi_i^-, \nu^- \leftarrow \phi_i, \nu$ ; replay  $\mathcal{B}$  stores  $(s, a, \tilde{r}, c, s', \tilde{\gamma}, \text{done})$ 
2: Init entropy temperature  $\alpha_{\text{ent}}$  (autotune with  $\mathcal{H}_{\text{tgt}} = -\dim(\mathcal{A})$  or fixed)
3: while training do
4:   Collect: sample  $a_t$  (random if  $t < t_{\text{learn}}$ , else  $a_t \sim \pi_\theta(\cdot|s_t)$ ); step env  $\rightarrow (r_t, c_t, s_{t+1}, \text{term}, \text{trunc})$ 
5:   if truncated, set  $s_{t+1} \leftarrow s_{t+1}^{\text{final}}$ ; set  $\text{done}_t \leftarrow \text{term}$ 
6:   Compute  $(\tilde{r}_t, \tilde{\gamma}_t)$ ; store  $(s_t, a_t, \tilde{r}_t, c_t, s_{t+1}, \tilde{\gamma}_t, \text{done}_t)$  in  $\mathcal{B}$ 
7:   if  $t \geq t_{\text{learn}}$  then
8:     Critic: sample batch from  $\mathcal{B}$ ; sample  $(a', \log \pi_\theta(a'|s'))$ ;
9:     set  $y = \tilde{r} + (1 - \text{done}) \tilde{\gamma} \min_i Q_{\phi_i^-}(s', a')$ 
10:    set  $z = \log \pi_\theta(a'|s') + \mathcal{H}_{\text{tgt}} + (1 - \text{done}) \tilde{\gamma} Q_{\nu^-}(s', a')$ 
11:    Update  $\phi_i$  by MSE to target  $y$  (with twin critics) and  $\nu$  to target  $z$ 
12:    Periodically update
13:      Actor:  $a_\pi \sim \pi_\theta(\cdot|s)$ ;  $\max_\theta \mathbb{E}[\min_i Q_{\phi_i}(s, a_\pi) - \kappa \{\log \pi_\theta(a_\pi|s) + Q_\nu(s, a_\pi)\}]$ 
14:      if autotune update  $\kappa$  using loss  $-\kappa Q_{\nu^-}(s', a')$ 
15:      update target critics:  $\phi_i^- \leftarrow \tau \phi_i + (1 - \tau) \phi_i^-$  and  $\nu^- \leftarrow \tau \nu + (1 - \tau) \nu^-$ 
16:      if CaT-scaler update violation scale:  $c_{\text{max}} \leftarrow \rho c_{\text{max}} + (1 - \rho)[c - b]_+$ 
17:    end if
18:  end while

```

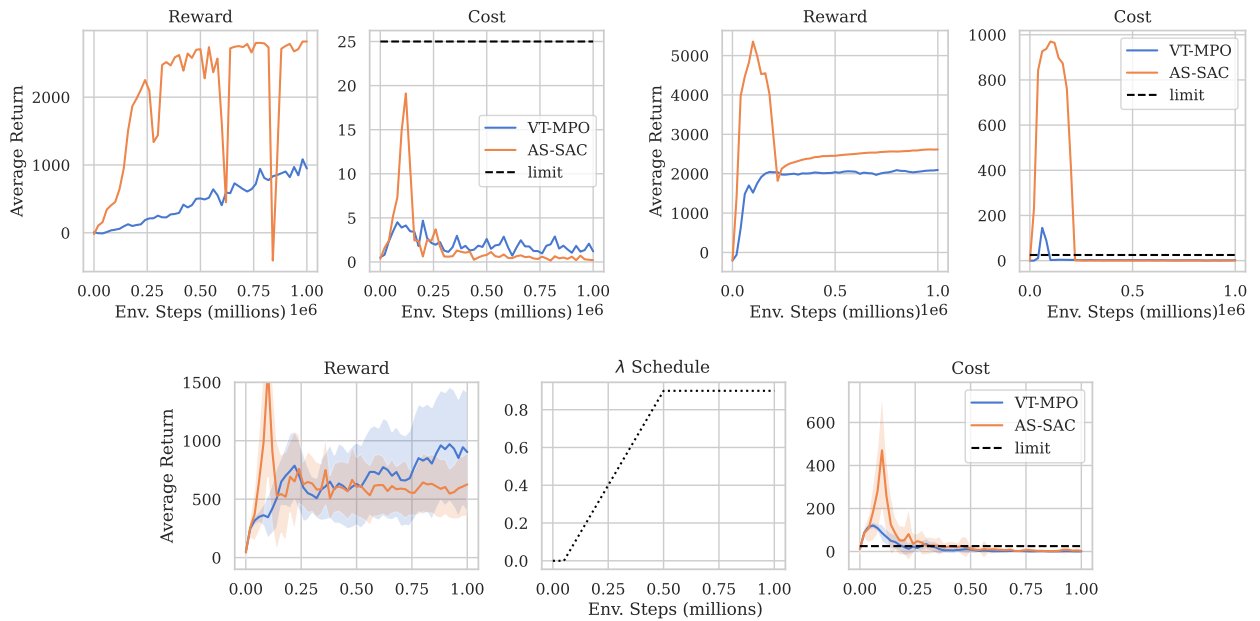
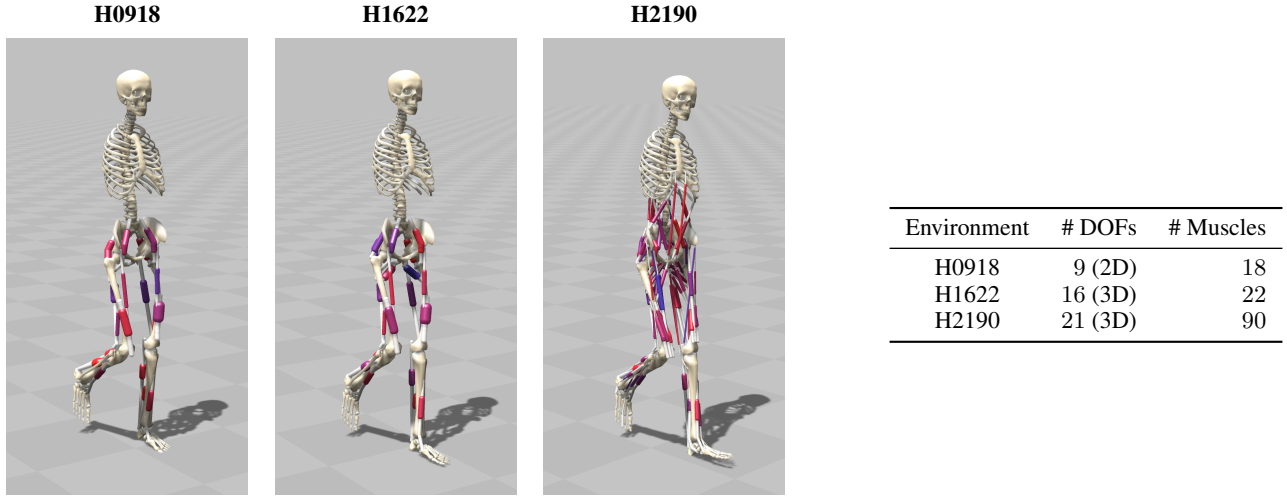


Figure 6. Results for AS-SAC and VT-MPO (individual seeds) on the Safety Gymnasium benchmark on the `AntVelocity` (top row, left) and `HalfCheetahVelocity` (top row, right) environments. The bottom row shows 5 seeds on the `HopperVelocity` environment and the linear schedule used for λ in the continuation probability $\alpha(s, a) = \exp(-\lambda c(s, a))$.

B.2. Experiments on Hyfydy

B.2.1. ENVIRONMENT OVERVIEW

The environments used are the H0918, H1622, and H2190 models from the biomechanical predictive simulation software Scione (Geijtenbeek, 2019). These simulations utilize the Hyfydy physics engine (Geijtenbeek, 2021), which implements high-fidelity physics and realistic muscle models optimized for the high throughput required in RL applications. We utilize these three models to evaluate VT-MPO across a spectrum of complexity: H0918 serves as a lower-dimensional testing ground, H1622 strikes a balance between realism and computational efficiency, and H2190 represents a high-complexity challenge with significantly higher degrees of freedom and muscle actuators. An overview of these models is provided in Figure 7.



(a) Considered musculoskeletal environments running on the Hyfydy engine (Geijtenbeek, 2021). Muscle actuators are visualized in red/purple. Complexity increases from left to right.

(b) Summary of Degrees of Freedom (DOFs) and muscle counts. The H0918 model is constrained to the sagittal plane (2D).

Figure 7. Hyfydy environment overview.

B.2.2. EFFORT WEIGHT ADAPTATION

Effort Weight Adaptation (EWA) (Schumacher et al., 2025) is a heuristic, MPO-based gait optimization algorithm designed to resolve the tension between minimizing effort and satisfying task-specific objectives, such as target velocity. It achieves this by dynamically adjusting the scalar weight α corresponding to the effort objective based on a moving average of the task return R_{mean} . The adaptation logic is detailed in Algorithm 4.

We categorize EWA as a *Lagrange-style* approach. Although it eschews formal dual descent in favor of a threshold-based heuristic, it is functionally equivalent to a dual update where the objective weight—the effective Lagrange multiplier—is modulated by constraint satisfaction (performance above threshold θ). This heuristic has proven highly effective for generating energy efficient gaits in musculoskeletal models.

Our work is motivated by the empirical success of such reweighting schemes in identifying viable trade-offs between effort and velocity in over-actuated systems. However, while EWA relies on a global, non-stationary weight that can lead to training oscillations, our proposed SDH formulation provides a principled probabilistic foundation. By moving the “reweighting” into the local state-action dependent continuation probability $\alpha(s, a)$, we transform the global switching logic of EWA into a smooth, survival-weighted objective.

Algorithm 4 Effort Weight Adaptation

Input: threshold θ , smoothing β , adaptation rate $\Delta\alpha$, decay rate λ

$R_{\text{mean}} \leftarrow 0, \alpha \leftarrow 0, c_{\text{mean}} \leftarrow 0$

for episodes $t = 0, 1, 2, \dots$ **do**

- $R \leftarrow \text{train_episode}()$ // Train and get return R
- $R_{\text{mean}} \leftarrow \beta R_{\text{mean}} + (1 - \beta)R$
- if** $R_{\text{mean}} > \theta$ **and** $c_{\text{mean}} < 0.5$ **then**

 - $\Delta\alpha \leftarrow \lambda\Delta\alpha$ // Convergence decay

- else if** $R_{\text{mean}} > \theta$ **and** $c_{\text{mean}} > 0.5$ **then**

 - $\alpha(t+1) \leftarrow \alpha(t) + \Delta\alpha$ // Increase effort pressure

- else**

 - $\alpha(t+1) \leftarrow \alpha(t) - \Delta\alpha$ // Relax effort pressure

- end if**
- $c_{\text{target}} \leftarrow \mathbb{I}(R_{\text{mean}} > \theta)$
- $c_{\text{mean}} \leftarrow \beta c_{\text{mean}} + (1 - \beta)c_{\text{target}}$

end for

B.2.3. EWA OBJECTIVE FORMULATION

For the EWA baseline, we employ a simplified objective formulation based on Schumacher et al. (2025), focusing exclusively on effort and velocity. The agent is trained with the reward:

$$r = r_{\text{vel}} - c_{\text{effort}}, \quad (5)$$

where the velocity reward r_{vel} is defined as:

$$r_{\text{vel}} = \begin{cases} \exp(-(v - v_{\text{target}})^2) & \text{if } v \leq v_{\text{target}} \\ 1 & \text{otherwise} \end{cases} \quad (6)$$

and the effort penalty is given by:

$$c_{\text{effort}} = \alpha(t) \left(N_{\text{muscles}}^{-1} \sum_{i=1}^{N_{\text{muscles}}} a_i^3 \right). \quad (7)$$

Here, $\alpha(t)$ represents the dynamically adjusted weight for policy effort, updated according to the procedure in Algorithm 4. a_i corresponds to the activation of the i -th muscle, and $v_{\text{target}} = 1.2 \text{ m s}^{-1}$. To ensure a fair comparison with VT-MPO, this baseline utilizes the same DEP exploration as described in Section B.2.4. The resulting training dynamics are visualized in Figure 4 (green curve). We observe that while the agent successfully learns a stable walking gait—as evidenced by the high episode length—the algorithm fails to effectively minimize effort in this simplified setting.

Notably, the original implementation of EWA achieves better energy efficiency by incorporating several domain-specific biomechanical penalties alongside velocity and muscle activations a . These include joint limit torques τ_i^{lim} , ground reaction forces F_j^{GRF} , muscle excitations u_i , and the number of active muscles N_{active} . We deliberately omit these auxiliary terms in our comparison to evaluate the fundamental ability of each algorithm to resolve the primary tension between velocity and effort. Relying on extensive reward shaping can mask the underlying stability issues of an optimizer; by using a reduced formulation, we provide a more rigorous test of how well the framework handles competing objectives in their rawest form. Our results suggest that while VT-MPO converges to efficient gaits under these minimal conditions, the EWA baseline may rely on the additional shaping terms to guide the optimization and prevent collapse.

B.2.4. SCALING VT-MPO TO HIGH-DIMENSIONAL MUSCULOSKELETAL CONTROL

In musculoskeletal control, energy efficiency is a desirable secondary objective that must be balanced against the primary requirement of locomotion: maintaining a target velocity. While standard RL often relies on the hand-engineered curricula and dynamic reweighting schemes discussed above, the SDH framework provides a mechanism to enforce this hierarchy through the planning horizon itself.

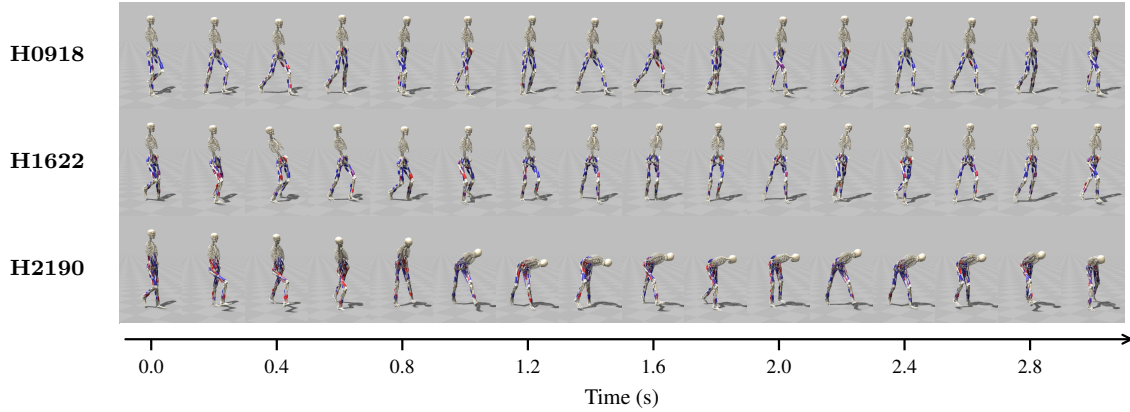


Figure 8. Unrolled gait visualizations for the H0918 (top), H1622 (middle), and H2190 (bottom) models. VT-MPO identifies robust gait patterns that maintain the velocity constraint under the stochastic horizon across all complexity levels. The forward-tilted gait observed in the H2190 model represents a stable local optimum for the simplified effort-velocity objective, which in works targeting gait realism, is typically avoided through extensive reward shaping. Because we do not include the auxiliary biomechanical penalties used in EWA (e.g., joint-limit or impact costs), the resulting motions are energy efficient but not human-like. The gaits developed here represent an important first step toward enabling more complex, realistic gait formulations in a principled framework.

In this setting, we incorporate the primary requirement (velocity tracking) into the continuation model $\alpha(s, a)$, while treating the secondary objective (effort minimization) as the principal reward. This formulation naturally prioritizes “survival”—defined here as remaining within the target velocity bounds—over energy savings. By localizing the constraint within the continuation probability, the policy is penalized for violations through a reduced effective horizon rather than a global, non-stationary weight.

We evaluate the scalability of VT-MPO across the three humanoid models of increasing complexity described in Section B.2.1. We focus on the VT-MPO variant due to its superior stability in high-dimensional locomotion tasks and to ensure a consistent comparison with the MPO-based EWA baseline. Unlike previous heuristic approaches, VT-MPO identifies viable biomechanical trade-offs without requiring Lagrange multipliers or adaptive dual scheme, relying solely on the intrinsic regularization of the survival-weighted return.

Hyfydy problem formulation and training setup. To evaluate VT-MPO in these complex systems, we solve a task we term *Walk to Survive*. Formulated as a CaI problem using the Batch-EMA scaling continuation model (recall Section 6.1), the objective is to maximize metabolic efficiency while treating velocity adherence as the fundamental survival constraint:

$$r(s, a) := 1 - \frac{1}{N_{\text{muscles}}} \sum_{i=0}^{N_{\text{muscles}}} \frac{a_i^3}{a_{\max}^3}, \quad (8)$$

$$c(s, a) := [v_{\text{target}} - v_x]_+, \quad (9)$$

where $v_{\text{target}} = 1.085 \text{ m s}^{-1}$ and $a_{\max} = 0.5$. Here, muscle activation a_i serves as a proxy for energy consumption. Consistent with literature on musculoskeletal modeling, we optimize for the 3rd power of activation as a form of reward shaping, but report the 2nd power in all subsequent plots to remain comparable with standard performance metrics (Schumacher et al., 2025).

Notably, we utilize a lower target velocity than the EWA baseline. This adjustment is necessary because VT-MPO optimizes for *worst-case* constraint satisfaction at every time step, whereas EWA utilizes a cumulative reward formulation; the lower threshold is therefore required to achieve rough parity in task difficulty and performance characteristics.

During training, we employ the stochastic-switch DEP exploration strategy (Schumacher et al., 2023). DEP exploration facilitates the discovery of complex gait patterns by intermittently switching to a controller that amplifies velocity correlations

across joints (the DEP controller), generating coordinated, large-scale exploratory movements that standard Gaussian noise cannot easily produce. The inclusion of DEP serves two purposes: first, it provides a high-quality exploration prior beneficial for learning locomotion; second, it stress-tests the off-policy robustness of the SDH framework (see Section B.2.5). To further stabilize the initial phase of learning, we schedule the termination probability $p_{\max}(t)$ in our continuation model:

$$p_{\max}(t) = p_{\text{end,max}} \cdot \min \left\{ \frac{t}{t_{\text{end,max}}}, 1 \right\}, \quad (10)$$

The quantitative training performance across all three musculoskeletal environments is shown in Figure 4, while the resulting gait patterns are visualized in Figure 8. Across all models, VT-MPO successfully learns to prioritize the survival-linked velocity objective, resulting in stable and robust locomotion.

B.2.5. VT-MPO DEP ABLATION EXPERIMENT

A central claim of the Stochastic Decision Horizon (SDH) framework is its compatibility with off-policy data—a property often lacking in constrained RL methods that rely on on-policy stationary assumptions. To verify that VT-MPO inherits the robust off-policy capabilities of MPO, we evaluate its performance on the high-dimensional H2190 task with and without the Differential Extrinsic Plasticity (DEP) exploration controller (Schumacher et al., 2023).

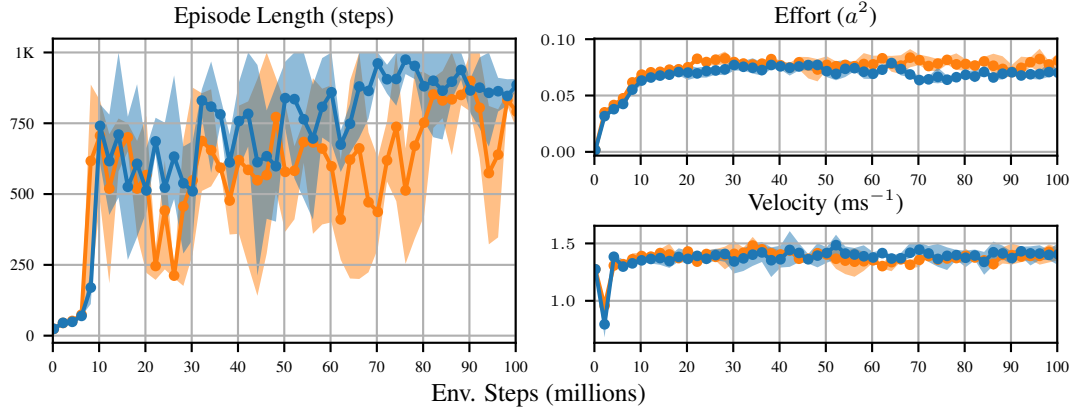


Figure 9. Ablation experiments for the off-policy exploration controller DEP on the H2190 environment. Shown are the average, minimum, and maximum metric values for 3 seeds of VT-MPO with DEP (●) and without DEP (○). The inclusion of DEP accelerates the reduction of effort requirements while maintaining consistently higher episode lengths. This confirms that VT-MPO effectively leverages highly off-policy exploration data to identify energy-efficient gait patterns.

As illustrated in Figure 9, VT-MPO not only remains stable when trained on partially DEP-generated data but actively benefits from it. The usage of DEP leads to more consistent episode lengths and a faster decrease in effort requirements. Because DEP’s correlated motions encourage the agent to explore valid mechanical interactions rather than high-frequency jitter, VT-MPO is able to identify feasible, low-effort transitions more rapidly.

Notably, this benefit is most pronounced in the high-dimensional H2190 model. In the lower-complexity H0918 and H1622 environments, the performance gap between DEP and standard Gaussian exploration is less significant. This is likely due to the lower levels of over-actuation in these models, where the search space is sufficiently constrained such that unstructured noise remains a viable—albeit less efficient—means of discovering stable gait patterns. In contrast, for the 90-muscle H2190 model, the robustness of the SDH framework to off-policy data becomes a critical asset, allowing it to leverage the structured, correlated exploration of DEP to navigate the vast null-space of the muscle redundancy.

B.2.6. SINGLE-SEED TRAINING DYNAMICS

To investigate the practical stability of the stochastic horizon formulation, we examine the training dynamics of individual seeds for VT-MPO on the high-dimensional H1622 walking task (Figure 10).

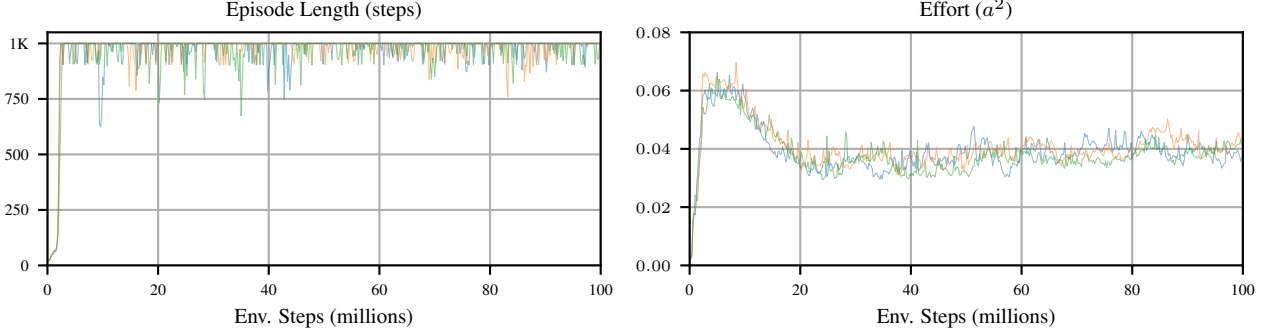


Figure 10. Single-seed training dynamics of VT-MPO on H1622. The curves show consistent convergence across independent runs toward a stable tradeoff between velocity adherence and energy efficiency.

The stability observed across seeds is particularly notable in high-dimensional musculoskeletal systems, where the coupling between policy updates and dual-variable adjustments in Lagrangian methods often proves difficult to stabilize. In such frameworks, the temporal lag between weight shifts and gait adaptations can trigger "limit cycles," where the agent alternates between aggressive effort minimization and performance recovery.

VT-MPO avoids this tuning challenge by localizing the violation penalty as an instantaneous reduction in the planning horizon. By encoding the constraint via the continuation probability $\alpha(s, a)$ directly within the Bellman update, the framework replaces the global, lagging logic of weight updates with smooth, survival-weighted credit assignment. The agent thus learns to balance effort and velocity within the MDP's temporal structure itself.

C. Control as Inference with Stochastic Decision Horizons

Consider an infinite-horizon discounted MDP $(\mathcal{S}, \mathcal{A}, P, r, \gamma)$ with $\gamma \in (0, 1)$. Fix a reference (prior) policy $\pi_0(a \mid s)$ and a candidate policy $\pi(a \mid s)$.

Geometric horizon for discounting. We use the standard geometric-horizon construction:

$$D_t \sim \text{Bernoulli}(1 - \gamma) \text{ i.i.d.}, \quad H_t := \prod_{k=0}^{t-1} (1 - D_k), \quad (11)$$

so that $H_t = 1$ iff the process has not stopped before acting at time t , and $\mathbb{E}[H_t] = \gamma^t$.

Feasibility / survival process. Introduce an additional Bernoulli variable

$$C_t \sim \text{Bernoulli}(\alpha(s_t, a_t)), \quad \alpha : \mathcal{S} \times \mathcal{A} \rightarrow [0, 1]. \quad (12)$$

Survival-to-reward gating. We use a *survival-to-reward* convention: the reward at time t contributes only if feasibility has held up to and including time t . Define

$$Z_t := \prod_{k=0}^{t-1} C_k, \quad \tilde{Z}_t := Z_t C_t = \prod_{k=0}^t C_k, \quad (13)$$

and the shared reward/optimality gate

$$\Gamma_t := H_t \tilde{Z}_t = H_t \prod_{k=0}^t C_k. \quad (14)$$

Thus $\Gamma_t = 1$ iff (i) the geometric horizon has not stopped before t and (ii) feasibility has held through t .

Two semantics: absorbing vs. virtual termination. We distinguish:

- **AS (absorbing state / real termination):** after the first $C_t = 0$, the controlled process stops generating actions (equivalently, transitions to an absorbing terminal state).
- **VT (virtual termination):** the controlled process continues generating actions until the geometric stop D , but feasibility only gates which reward/likeness terms contribute.

Crucially, *AS vs. VT differ only in which time steps exist as decisions for the KL term, not in the survival-to-reward convention (which is always governed by Γ_t)*. To unify notation, define the decision-existence indicators

$$A_t^{\text{AS}} := H_t \prod_{k=0}^{t-1} C_k, \quad A_t^{\text{VT}} := H_t. \quad (15)$$

Operational consequence. AS and VT share the same survival-weighted reward term (because Γ_t is shared), but VT continues to generate actions after feasibility failure and therefore continues to accumulate a KL/log-ratio penalty on those actions (Thm. C.1). As a result, post-failure behavior can affect the optimizer under VT unless the policy is forced (or able) to match π_0 after failure.

C.1. Control as Inference model

Define the generative model p and variational model q as

$$p(\tau, C, D) = p(s_0) \prod_{t \geq 0} \left[\pi_0(a_t \mid s_t) P(s_{t+1} \mid s_t, a_t) p(C_t \mid s_t, a_t) p(D_t) \right], \quad (16)$$

$$q(\tau, C, D) = p(s_0) \prod_{t \geq 0} \left[\pi(a_t \mid s_t) P(s_{t+1} \mid s_t, a_t) p(C_t \mid s_t, a_t) p(D_t) \right], \quad (17)$$

where $p(C_t = 1 \mid s_t, a_t) = \alpha(s_t, a_t)$ and $p(D_t)$ is as in (11). Let the (unnormalized) optimality *potential* be the gated factor³

$$p(O = 1 \mid \tau, C, D) := \exp\left(\frac{1}{\kappa} \sum_{t \geq 0} \Gamma_t r(s_t, a_t)\right), \quad \kappa > 0. \quad (18)$$

C.2. Two ELBO objectives and main result

Define the scaled ELBO objective

$$\mathcal{J}(\pi) := \kappa \cdot \mathbb{E}_q \left[\log p(O = 1 \mid \tau, C, D) \right] - \kappa \cdot D_{\text{KL}}(q(\tau, C, D) \parallel p(\tau, C, D)). \quad (19)$$

Using (18), this is exactly

$$\mathcal{J}(\pi) = \mathbb{E}_q \left[\sum_{t \geq 0} \Gamma_t r(s_t, a_t) \right] - \kappa D_{\text{KL}}(q(\tau, C, D) \parallel p(\tau, C, D)). \quad (20)$$

The following theorem gives closed-form expressions for $\mathcal{J}(\pi)$ under the AS and VT semantics as expectations over trajectories induced by π .

Theorem C.1 (Exact objectives for CaI+AS and CaI+VT). *It holds that*

$$\mathcal{J}_{\text{AS}}(\pi) = \mathbb{E}_{\tau \sim \pi} \left[\sum_{t \geq 0} \gamma^t \left(\prod_{k=0}^t \alpha_k \right) r_t - \kappa \sum_{t \geq 0} \gamma^t \left(\prod_{k=0}^{t-1} \alpha_k \right) \log \frac{\pi(a_t \mid s_t)}{\pi_0(a_t \mid s_t)} \right], \quad (21)$$

$$\mathcal{J}_{\text{VT}}(\pi) = \mathbb{E}_{\tau \sim \pi} \left[\sum_{t \geq 0} \gamma^t \left(\prod_{k=0}^t \alpha_k \right) r_t - \kappa \sum_{t \geq 0} \gamma^t \log \frac{\pi(a_t \mid s_t)}{\pi_0(a_t \mid s_t)} \right], \quad (22)$$

where $\alpha_k \equiv \alpha(s_k, a_k)$ and $r_t \equiv r(s_t, a_t)$.

Proof overview. The reward term is shared across AS/VT because it is gated by Γ_t (Lem. C.3). The only difference is the KL term, which is gated by the decision-existence indicator A_t (Lem. C.2). A full, detailed proof is given in App. C.4.

C.3. Supporting lemmas

Lemma C.2 (Trajectory KL reduces to a gated sum of log policy ratios). *For either semantics, the only difference between $q(\tau, C, D)$ and $p(\tau, C, D)$ is π vs. π_0 , hence*

$$D_{\text{KL}}(q(\tau, C, D) \parallel p(\tau, C, D)) = \mathbb{E}_q \left[\sum_{t \geq 0} A_t \log \frac{\pi(a_t \mid s_t)}{\pi_0(a_t \mid s_t)} \right], \quad (23)$$

where $A_t = A_t^{\text{AS}}$ under AS and $A_t = A_t^{\text{VT}}$ under VT.

Proof. By definition,

$$D_{\text{KL}}(q \parallel p) = \mathbb{E}_q \left[\log \frac{q(\tau, C, D)}{p(\tau, C, D)} \right]. \quad (24)$$

Using the factorizations (16)–(17), the ratio q/p telescopes:

$$\begin{aligned} \log \frac{q(\tau, C, D)}{p(\tau, C, D)} &= \sum_{t \geq 0} \log \frac{\pi(a_t \mid s_t)}{\pi_0(a_t \mid s_t)} + \sum_{t \geq 0} \log \frac{P(s_{t+1} \mid s_t, a_t)}{P(s_{t+1} \mid s_t, a_t)} + \sum_{t \geq 0} \log \frac{p(C_t \mid s_t, a_t)}{p(C_t \mid s_t, a_t)} + \sum_{t \geq 0} \log \frac{p(D_t)}{p(D_t)} \\ &= \sum_{t \geq 0} \log \frac{\pi(a_t \mid s_t)}{\pi_0(a_t \mid s_t)}, \end{aligned} \quad (25)$$

³Following standard Control as Inference notation, $p(O=1 \mid \tau, C, D)$ denotes an *unnormalized* nonnegative factor (potential/energy), not a normalized conditional probability. All variational bounds below are understood as bounds on the log-normalizer of the corresponding unnormalized joint $\tilde{p}(\tau, C, D, O=1) := p(\tau, C, D) p(O=1 \mid \tau, C, D)$.

where all non-policy terms cancel exactly.

What remains is to account for which indices t correspond to *actual* action draws under each semantics. Equivalently, we multiply each summand by the indicator that a decision at time t exists. By construction, this indicator is precisely A_t :

- Under **AS**, decisions exist iff the geometric horizon has not stopped before t *and* feasibility has not failed before t , i.e. $A_t^{\text{AS}} = H_t \prod_{k=0}^{t-1} C_k$.
- Under **VT**, decisions exist iff the geometric horizon has not stopped before t , independent of feasibility, i.e. $A_t^{\text{VT}} = H_t$.

Thus,

$$\log \frac{q(\tau, C, D)}{p(\tau, C, D)} = \sum_{t \geq 0} A_t \log \frac{\pi(a_t | s_t)}{\pi_0(a_t | s_t)}. \quad (26)$$

Taking $\mathbb{E}_q[\cdot]$ and using (24) yields the claim. \square

Lemma C.3 (Conditional expectations of gates). *Condition on a realized state-action sequence $\tau = (s_0, a_0, s_1, a_1, \dots)$. Then for both semantics,*

$$\mathbb{E}[\Gamma_t | \tau] = \gamma^t \prod_{k=0}^t \alpha(s_k, a_k), \quad (27)$$

and for the decision-existence indicators,

$$\mathbb{E}[A_t^{\text{AS}} | \tau] = \gamma^t \prod_{k=0}^{t-1} \alpha(s_k, a_k), \quad \mathbb{E}[A_t^{\text{VT}} | \tau] = \gamma^t. \quad (28)$$

Proof. Fix τ . Under the model, conditional on τ the random variables $\{C_k\}_{k \geq 0}$ are independent with

$$\mathbb{E}[C_k | \tau] = \Pr(C_k = 1 | s_k, a_k) = \alpha(s_k, a_k) =: \alpha_k, \quad (29)$$

and $\{D_k\}_{k \geq 0}$ are i.i.d. Bernoulli($1 - \gamma$), independent of $\{C_k\}$ and of τ .

Geometric survival factor. By definition $H_t = \prod_{k=0}^{t-1} (1 - D_k)$, and $(1 - D_k) \in \{0, 1\}$ with $\mathbb{E}[1 - D_k] = \Pr(D_k = 0) = \gamma$. Independence across k gives

$$\mathbb{E}[H_t] = \prod_{k=0}^{t-1} \mathbb{E}[1 - D_k] = \gamma^t. \quad (30)$$

Reward/optimality gate. Recall $\Gamma_t = H_t \prod_{k=0}^t C_k$. Using independence of H_t and $\{C_k\}$ and independence of the C_k 's conditional on τ ,

$$\mathbb{E}[\Gamma_t | \tau] = \mathbb{E}[H_t] \prod_{k=0}^t \mathbb{E}[C_k | \tau] = \gamma^t \prod_{k=0}^t \alpha_k, \quad (31)$$

where we used (30) and (29).

Decision-existence indicators. For AS, $A_t^{\text{AS}} = H_t \prod_{k=0}^{t-1} C_k$, hence

$$\mathbb{E}[A_t^{\text{AS}} | \tau] = \mathbb{E}[H_t] \prod_{k=0}^{t-1} \mathbb{E}[C_k | \tau] = \gamma^t \prod_{k=0}^{t-1} \alpha_k. \quad (32)$$

For VT, $A_t^{\text{VT}} = H_t$, so $\mathbb{E}[A_t^{\text{VT}} | \tau] = \mathbb{E}[H_t] = \gamma^t$ by (30). \square

C.4. Proof of Thm. C.1

Proof. We start from a variational lower bound on the log-normalizer (evidence) of the *unnormalized* joint $\tilde{p}(\tau, C, D, O=1) = p(\tau, C, D) p(O=1 | \tau, C, D)$. For any $q(\tau, C, D)$,

$$\begin{aligned} \log \tilde{p}(O=1) &= \log \int \sum_{C,D} q(\tau, C, D) \frac{p(\tau, C, D) p(O=1 | \tau, C, D)}{q(\tau, C, D)} d\tau \\ &\geq \mathbb{E}_q \left[\log p(O=1 | \tau, C, D) \right] - D_{\text{KL}}(q(\tau, C, D) \| p(\tau, C, D)). \end{aligned} \quad (33)$$

Since by (18)

$$\log p(O=1 | \tau, C, D) = \frac{1}{\kappa} \sum_{t \geq 0} \Gamma_t r_t, \quad (34)$$

multiplying the ELBO by $\kappa > 0$ yields the scaled objective (20):

$$\mathcal{J}(\pi) = \mathbb{E}_q \left[\sum_{t \geq 0} \Gamma_t r_t \right] - \kappa D_{\text{KL}}(q(\tau, C, D) \| p(\tau, C, D)). \quad (20 \text{ revisited})$$

Step 1: Reward term. Use the tower property conditioning on the (state, action) trajectory τ :

$$\mathbb{E}_q \left[\sum_{t \geq 0} \Gamma_t r_t \right] = \mathbb{E}_{\tau \sim \pi} \left[\sum_{t \geq 0} \mathbb{E}[\Gamma_t | \tau] r_t \right]. \quad (35)$$

By Lem. C.3,

$$\mathbb{E}[\Gamma_t | \tau] = \gamma^t \prod_{k=0}^t \alpha_k, \quad (36)$$

so

$$\mathbb{E}_q \left[\sum_{t \geq 0} \Gamma_t r_t \right] = \mathbb{E}_{\tau \sim \pi} \left[\sum_{t \geq 0} \gamma^t \left(\prod_{k=0}^t \alpha_k \right) r_t \right]. \quad (37)$$

Step 2: KL term (AS vs. VT differs here). By Lem. C.2,

$$\begin{aligned} D_{\text{KL}}(q \| p) &= \mathbb{E}_q \left[\sum_{t \geq 0} A_t \log \frac{\pi(a_t | s_t)}{\pi_0(a_t | s_t)} \right] \\ &= \mathbb{E}_{\tau \sim \pi} \left[\sum_{t \geq 0} \mathbb{E}[A_t | \tau] \log \frac{\pi(a_t | s_t)}{\pi_0(a_t | s_t)} \right], \end{aligned} \quad (38)$$

where the second line is the tower property.

AS case. By Lem. C.3,

$$\mathbb{E}[A_t^{\text{AS}} | \tau] = \gamma^t \prod_{k=0}^{t-1} \alpha_k, \quad (39)$$

hence

$$D_{\text{KL}}(q \| p) = \mathbb{E}_{\tau \sim \pi} \left[\sum_{t \geq 0} \gamma^t \left(\prod_{k=0}^{t-1} \alpha_k \right) \log \frac{\pi(a_t | s_t)}{\pi_0(a_t | s_t)} \right]. \quad (40)$$

VT case. Again by Lem. C.3,

$$\mathbb{E}[A_t^{\text{VT}} | \tau] = \gamma^t, \quad (41)$$

so

$$D_{\text{KL}}(q \| p) = \mathbb{E}_{\tau \sim \pi} \left[\sum_{t \geq 0} \gamma^t \log \frac{\pi(a_t | s_t)}{\pi_0(a_t | s_t)} \right]. \quad (42)$$

Step 3: Combine reward and KL. Substituting (37) and (40) into (20) yields (21). Substituting (37) and (42) into (20) yields (22). This proves the theorem. \square

C.5. Bellman operators and contraction

For an arbitrary function $f(s, a)$, we generalize the variable-discount evaluation recursion using the following transformations:

$$\tilde{r}(s, a) := \alpha(s, a)r(s, a) + f(s, a), \quad \tilde{\gamma}(s, a) := \gamma \alpha(s, a).$$

Assumption C.4 (Boundedness). Rewards are bounded: $|r(s, a)| \leq R_{\max}$, and $\tilde{\gamma}(s, a) \in [0, \gamma]$ for all (s, a) .

Definition C.5 (Variable-discount evaluation operator). Fix a policy π . For any bounded $V : \mathcal{S} \rightarrow \mathbb{R}$, define

$$(\mathcal{T}_{\tilde{r}, \tilde{\gamma}}^\pi V)(s) := \mathbb{E}_{a \sim \pi(\cdot|s)} \left[\tilde{r}(s, a) + \tilde{\gamma}(s, a) \mathbb{E}_{s' \sim P(\cdot|s, a)} V(s') \right]. \quad (43)$$

Note that this framework generalizes both the regularized and unregularized survival-weighted operators presented in the main text. Specifically, we recover the respective operators by setting $\tilde{\gamma}(s, a) = \gamma\alpha(s, a)$ and defining the reward for (Absorbing State) $\tilde{r}_{\text{AS}}(s, a) = \alpha(s, a)r(s, a) - \log \pi(a|s)$ and (Virtual Termination) $\tilde{r}_{\text{VT}}(s, a) = \alpha(s, a)r(s, a)$.

Lemma C.6 (Contraction). *Under Assumption C.4, $\mathcal{T}_{\tilde{r}, \tilde{\gamma}}^\pi$ is a γ -contraction in the sup norm:*

$$\|\mathcal{T}_{\tilde{r}, \tilde{\gamma}}^\pi V - \mathcal{T}_{\tilde{r}, \tilde{\gamma}}^\pi W\|_\infty \leq \gamma \|V - W\|_\infty.$$

Consequently, $\mathcal{T}_{\tilde{r}, \tilde{\gamma}}^\pi$ has a unique fixed point V^π , and $(\mathcal{T}_{\tilde{r}, \tilde{\gamma}}^\pi)^n V$ converges to V^π for any bounded initialization V .

Proof. Fix bounded V, W and any $s \in \mathcal{S}$. By definition (43),

$$\begin{aligned} |(\mathcal{T}_{\tilde{r}, \tilde{\gamma}}^\pi V)(s) - (\mathcal{T}_{\tilde{r}, \tilde{\gamma}}^\pi W)(s)| &= \left| \mathbb{E}_{a \sim \pi(\cdot|s)} \left[\tilde{\gamma}(s, a) \mathbb{E}_{s' \sim P(\cdot|s, a)} (V(s') - W(s')) \right] \right| \\ &\leq \mathbb{E}_{a \sim \pi(\cdot|s)} \left[\tilde{\gamma}(s, a) \mathbb{E}_{s'} |V(s') - W(s')| \right] \\ &\leq \mathbb{E}_{a \sim \pi(\cdot|s)} [\tilde{\gamma}(s, a)] \|V - W\|_\infty \\ &\leq \gamma \|V - W\|_\infty, \end{aligned} \quad (44)$$

where we used $\tilde{\gamma}(s, a) \in [0, \gamma]$ (Assumption C.4). Taking the supremum over s yields the contraction inequality. The existence and uniqueness of the fixed point and convergence of iterates follow from the Banach fixed point theorem. \square

D. Relation to Constrained RL and Related Frameworks

This section serves three purposes: (i) it shows how prior termination-style returns are recovered as special cases of the general SDH continuation model; (ii) it states a finite-horizon certificate-style chance bound under exponential continuation; and (iii) it discusses potential connections between SDH and constrained MDPs.

Stochastic Decision Horizons (SDH). SDH is the general modeling device of a *state-action-dependent continuation probability* $\alpha : \mathcal{S} \times \mathcal{A} \rightarrow [0, 1]$ in Control as Inference. It induces a *survival gate* $Z_t := \prod_{k=0}^t \alpha(s_k, a_k)$ and the associated survival-weighted return

$$J_{\text{surv}}(\pi) := \mathbb{E}_{\tau \sim \pi} \left[\sum_{t \geq 0} \gamma^t Z_t r(s_t, a_t) \right]. \quad (45)$$

Equivalently, SDH corresponds to control in an MDP with shaped reward $\tilde{r}(s, a) = \alpha(s, a)r(s, a)$, state-action-dependent discount $\tilde{\gamma}(s, a) = \gamma\alpha(s, a)$, and (shaped) entropy regularization (cf. main text). The termination-style objective Eq. 45 can be paired with different semantics for what happens *after* a violation: (i) **absorbing state** (AS) semantics, where termination ends the decision process and *both* reward and any regularization (e.g., KL) stop accumulating; and (ii) **virtual termination** (VT) semantics, where the agent continues acting but the model only gates which reward/likelihood terms contribute to trajectory optimality. These semantics share the same survival-weighted return but differ in how information costs are accumulated (cf. Prop. 4.1 / Thm. C.1).

How SDH differs from termination-style returns. SDH is a generalization of termination-style frameworks for constrained MDPs, in particular Early Terminated MDP (ET-MDP) introduced by Sun et al. (2022) and Constraints as Terminations (CaT) by Chane-Sane et al. (2024). Both can be seen as particular *design choices* for α constructed from constraint signals via a termination probability: $\alpha(s, a)$ can be binary or smooth, hand-designed or learned, and is not tied to any specific algorithmic mechanism beyond shaping credit assignment through $(\tilde{r}, \tilde{\gamma})$. In contrast to these frameworks, SDH reconciles the survival-shaped return with entropy regularization in RL and distinguishes two termination semantics (AS vs. VT), which affect KL accumulation but not the shared survival return.

D.1. Notation and setup

We consider an infinite-horizon discounted MDP $(\mathcal{S}, \mathcal{A}, \mathcal{P}, r, \gamma)$ with discount factor $\gamma \in (0, 1)$ and trajectories $\tau = (s_0, a_0, s_1, a_1, \dots)$ generated by a policy π and dynamics \mathcal{P} . At each step we observe reward $r(s_t, a_t)$ and a collection of constraint functions $\{c_i : \mathcal{S} \times \mathcal{A} \rightarrow \mathbb{R}\}_{i \in I}$, where a violation occurs when $c_i(s_t, a_t) > 0$.

Following the notation in Chane-Sane et al. (2024), CaT introduces a *termination probability* $\delta : \mathcal{S} \times \mathcal{A} \rightarrow [0, 1]$ (potentially increasing with constraint violation magnitude) and the associated *continuation probability*

$$\alpha(s, a) := 1 - \delta(s, a) \in [0, 1],$$

with $\delta_t := \delta(s_t, a_t)$ and $\alpha_t := \alpha(s_t, a_t)$. The induced survival gate up to time t is $\prod_{k=0}^t \alpha_k$, which down-weights rewards after infeasible behavior. In the hard (binary) case, $\delta(s, a) = 1 - \prod_{i \in I} \mathbf{1}\{c_i(s, a) \leq 0\}$ so that $\alpha(s, a) \in \{0, 1\}$ encodes whether all constraints are satisfied at (s, a) .

D.2. Relation to termination-style returns

CaT can be viewed as a particular *parameterization* of the general SDH continuation model $\alpha(s, a)$. Both CaT and SDH induce the same survival gate $\prod_{k \leq t} \alpha_k$. SDH decouples this modeling choice from a specific algorithmic instantiation (e.g., on-policy PPO), and allows exact entropy regularized objectives under AS/VT semantics.

CaT. CaT replaces additive budgeting by terminating credit assignment and optimizes a *survival-weighted* return

$$J_{\text{CaT}}(\pi) := \mathbb{E}_{\tau \sim \pi} \left[\sum_{t \geq 0} \gamma^t \left(\prod_{k=0}^t (1 - \delta(s_k, a_k)) \right) r(s_t, a_t) \right]. \quad (46)$$

Note that $J_{\text{CaT}}(\pi)$ is exactly $J_{\text{surv}}(\pi)$ from (45) under the identification $\alpha = 1 - \delta$. While the returns are equivalent, the full SDH objectives further involve two distinct types of entropy regularization given a choice of termination semantics (cf. main text).

ET-MDP. If the survival return is derived from a *binary* termination based on constraint satisfaction,

$$\delta(s, a) = 1 - \prod_{i \in I} \mathbf{1}\{c_i(s, a) \leq 0\}, \quad \text{i.e.} \quad \alpha(s, a) = \prod_{i \in I} \mathbf{1}\{c_i(s, a) \leq 0\}, \quad (47)$$

then $\alpha_t \in \{0, 1\}$ and the product $\prod_{k \leq t} \alpha_k$ becomes the indicator that no violation has occurred up to time t . Equivalently, letting the first violation time be

$$T := \inf \left\{ t \geq 0 : \max_{i \in I} c_i(s_t, a_t) > 0 \right\} \in \{0, 1, 2, \dots\} \cup \{\infty\},$$

we obtain the early terminated return

$$J_{\text{ET}}(\pi) = \mathbb{E}_{\tau \sim \pi} \left[\sum_{t=0}^{T-1} \gamma^t r(s_t, a_t) \right], \quad (48)$$

i.e., reward is accumulated only strictly before the first violation, which is the mechanism used in ET-MDP. In general, any continuation probability $\alpha \in (0, 1)$ can be seen as a relaxation of the ET-MDP formulation: constraint violations no longer deterministically truncate credit assignment, but progressively suppress it through $\prod_{k \leq t} \alpha_k$.

D.3. Additive hazard and a finite-horizon chance bound for exponential continuation

SDH couples constraint sensitivity through *products* of continuation probabilities. For analysis and monitoring it is convenient to work with an additive surrogate.

Lemma D.1 (Additive hazard representation). *Assume continuation $\alpha(s, a) \in (0, 1]$ and define the per-step hazard $h(s, a) := -\log \alpha(s, a) \in [0, \infty)$. Then for any horizon $H \geq 1$,*

$$\prod_{t=0}^{H-1} \alpha_t = \exp\left(-\sum_{t=0}^{H-1} h(s_t, a_t)\right).$$

Proof. Immediate from $\prod_t \alpha_t = \exp(\sum_t \log \alpha_t) = \exp(-\sum_t h_t)$. \square

We now specialize to the exponential continuation commonly used for safety shaping.

Assumption D.2 (Exponential continuation and cumulative cost). Let $c(s, a) \geq 0$ be a per-step violation magnitude and set

$$\alpha_\lambda(s, a) = \exp(-\lambda c(s, a)) \quad \text{for } \lambda > 0.$$

Define the finite-horizon cumulative cost $C_H := \sum_{t=0}^{H-1} c(s_t, a_t)$ and the SDH survival statistic

$$S_H(\lambda) := \mathbb{E}_{\tau \sim \pi} \left[\prod_{t=0}^{H-1} \alpha_\lambda(s_t, a_t) \right] = \mathbb{E}_{\tau \sim \pi} [e^{-\lambda C_H}].$$

Proposition D.3 (Exponential continuation induces a multiplicative (risk-sensitive) surrogate). *Under Assumption D.2, define the prefix cumulative cost*

$$C_{t+1} := \sum_{k=0}^t c(s_k, a_k).$$

Then the SDH/CaT survival-weighted return can be written as

$$J_{\text{surv}}(\pi) = \mathbb{E}_{\tau \sim \pi} \left[\sum_{t \geq 0} \gamma^t \exp(-\lambda C_{t+1}) r(s_t, a_t) \right],$$

which is a multiplicative (hazard / risk-sensitive) criterion that discounts reward by accumulated violation magnitude. In general, optimizing this surrogate is not equivalent to solving additive-cost chance-constrained CMDPs.

Proof. By Lem. D.1 and $\alpha_\lambda(s, a) = \exp(-\lambda c(s, a))$, $\prod_{k=0}^t \alpha_k = \exp(-\lambda \sum_{k=0}^t c_k) = \exp(-\lambda C_{t+1})$, and substitution into the definition of J_{surv} yields the claim. \square

Theorem D.4 (Finite-horizon chance upper bound via $S_H(\lambda)$). *Under Assumption D.2, for any horizon $H \geq 1$ and threshold $b > 0$,*

$$\mathbb{P}_\pi(C_H \geq b) \leq \frac{1 - S_H(\lambda)}{1 - e^{-\lambda b}}. \quad (49)$$

Proof. Consider the bounded random variable $Y := 1 - e^{-\lambda C_H} \in [0, 1]$. If $C_H \geq b$ then $e^{-\lambda C_H} \leq e^{-\lambda b}$ and hence $Y \geq 1 - e^{-\lambda b}$. Therefore,

$$\mathbb{P}_\pi(C_H \geq b) = \mathbb{P}_\pi(Y \geq 1 - e^{-\lambda b}).$$

By Markov's inequality for non-negative random variables, $\mathbb{P}(Y \geq a) \leq \mathbb{E}[Y]/a$ for any $a > 0$, giving

$$\mathbb{P}_\pi(C_H \geq b) \leq \frac{\mathbb{E}_\pi[Y]}{1 - e^{-\lambda b}} = \frac{1 - \mathbb{E}_\pi[e^{-\lambda C_H}]}{1 - e^{-\lambda b}} = \frac{1 - S_H(\lambda)}{1 - e^{-\lambda b}}.$$

\square

Corollary D.5 (Binary violations: bounding “any violation within H ”). *If $c(s, a) \in \{0, 1\}$ is a binary violation indicator, then $C_H \geq 1$ iff $\exists t < H$ with $c(s_t, a_t) = 1$. Thus Thm. D.4 with $b = 1$ yields*

$$\mathbb{P}_\pi(\exists t < H : c(s_t, a_t) = 1) \leq \frac{1 - S_H(\lambda)}{1 - e^{-\lambda}}.$$

Interpretation. Thm. D.4 yields an *upper bound* on the finite-horizon chance event $\{C_H \geq b\}$ that can be *reported* from rollouts by estimating $S_H(\lambda) = \mathbb{E}[e^{-\lambda C_H}]$. This does not mean SDH *solves* a chance-constrained MDP; rather, it provides a lightweight certificate-style statistic that connects an exponential continuation design choice to an explicit probabilistic upper bound.

AS vs. VT. The bounds above depend only on the shared survival gate $\prod_{k < H} \alpha_k$ and therefore apply to both CaI+AS and CaI+VT. The distinction between AS and VT affects how information costs (KL regularization) are accumulated (Prop. 4.1 / Thm. C.1), but not the survival statistic used in the chance bound.

D.4. Relation to chance constraints

While the bound in Thm. D.4 does not constitute a general feasibility guarantee, it provides a useful diagnostic for approximately tuning exponential continuation to a chance-constrained MDP. However, maximizing the survival return is not equivalent to solving a chance-constrained MDP in general. Establishing conditions under which SDH aligns with chance-constraints or almost-sure feasibility remains an open and promising direction, likely requiring additional structural assumptions such as terminal penalties or reward-scale constraints.

For example, Sun et al. (2022) show that maximizing the early-terminated return in Eq. (48) is equivalent to solving a finite-horizon constrained MDP under suitable terminal reward assumptions. Since ET-MDP is a special case of SDH, and given the chance bounds derived above, analogous results for SDH may be attainable under similar conditions, which we leave for future work.

E. Algorithmic Details

This section collects *only* the engineering/implementation points that are shared across methods and are not already spelled out in App. F (VT-MPO details) and App. G (AS-SAC and uniform-prior structure). In particular, we avoid restating MPO’s E/M steps, the definition of the survival critic, or the AS two-critic decomposition.

Unifying viewpoint (what changes and what does not). Across all SDH-based variants, constraints enter learning solely through a continuation probability $\alpha(s, a) \in [0, 1]$ computed from constraint signals, inducing shaped quantities

$$\tilde{r}(s, a) = \alpha(s, a) r(s, a), \quad \tilde{\gamma}(s, a) = \gamma \alpha(s, a),$$

which appear *only* in critic targets. Replay, target networks, and actor-side updates (SAC or MPO) are otherwise unchanged. AS vs. VT is a semantic distinction of the CaI objective that affects how information costs are accumulated (main text), but the continuation model α and survival gate used for shaping are shared.

E.1. Environment termination and `done` handling

In our experiments, constraint events do *not* reset the simulator; “termination” is objective-level through $\alpha(s, a)$. Episodes end only when the environment returns `done`.

True terminals vs. time limits. For critic bootstrapping we follow standard off-policy practice:

- for true terminal transitions, we disable bootstrapping with $(1 - \text{done})$ (so $\tilde{\gamma} = (1 - \text{done})\gamma\alpha$);
- for time-limit truncations, we allow bootstrapping via the usual timeout mask (absorbed into `done` in notation).

E.2. Continuation models used in the experiments

The theory requires only $\alpha(s, a) \in [0, 1]$. In practice, the choice of α is a modeling decision that controls how aggressively violations shorten the effective horizon and can materially affect off-policy stability. We use two simple mappings aligned with the regimes in our benchmarks.

Exponential continuation (Safety Gymnasium). Given per-step violation magnitudes $c_i(s, a) \geq 0$, we use the smooth attenuation

$$\alpha_{\text{exp}}(s, a) := \exp\left(-\lambda \sum_{i \in I} c_i(s, a)\right) \in (0, 1], \quad (50)$$

which avoids discontinuities and yields stable critic targets under replay. This continuation is used for both AS-SAC and VT-MPO on Safety Gymnasium.

CaT-style normalized continuation with saturation and batch-EMA scaling (Hyfydy). In Hyfydy, constraint magnitudes can have heterogeneous units/scales and can spike under exploration, so we use a normalized, saturating hazard. For a scalar cost signal $c(s, a) \geq 0$ (or violation magnitude after subtracting a limit), define

$$\alpha_{\text{CaT}}(s, a) := 1 - p^{\max} \text{clip}\left(\frac{c(s, a)}{\max(c_{\max}, \varepsilon)}, 0, 1\right), \quad (51)$$

with $\varepsilon > 0$ and cap $p^{\max} \in (0, 1]$. The scale c_{\max} is updated periodically from replay batches using an Exponential Moving Average (EMA) of the batch maximum violation magnitude:

$$c_{\max} \leftarrow \rho c_{\max} + (1 - \rho) \max_{c \in \mathcal{B}} [c - b]_+.$$

With multiple constraints, we compute α_i per constraint and aggregate via $\alpha = \min_i \alpha_i$.

E.3. Replay-format note for VT-MPO

VT-MPO uses a compressed TD(n) replay format that stores the precomputed survival-shaped n -step return and the single bootstrapping continuation factor. The full definitions and the resulting TD(n) target are given in App. F.3. We highlight one practical implication:

Off-policy corrections. Because compressed TD(n) does not retain per-step behavior-action information, sequence-based corrections (e.g. Retrace) are not directly applicable in this format. We therefore use uncorrected TD(n) regression on survival-shaped targets, which was stable in our settings (Sec. 6).

E.4. Where to find method-specific details

To keep the appendix consistent and non-redundant, we place the method-specific algorithmics in dedicated sections:

- **VT-MPO:** survival critic definition, unchanged MPO E/M steps, and variable-discount TD(n) targets are in App. F.
- **AS-SAC:** uniform-prior living-cost structure, soft Bellman recursion under $(\tilde{r}, \tilde{\gamma})$, two-critic decomposition, and κ dual update are in App. G.

This section summarizes the SDH-specific implementation interface required for replay-based off-policy learning: compute the continuation $\alpha(s, a)$ from constraint signals, apply survival shaping in critic targets via $(\tilde{r}, \tilde{\gamma})$, and treat environment termination (`done`) with standard bootstrapping masks. All remaining components of the optimization (SAC-style actor/temperature updates under AS and MPO E/M steps under VT) are unchanged and described in the corresponding appendices.

F. VT-MPO: MPO with a Survival-Shaped Critic

This section specifies the only deviation from standard MPO: we keep MPO’s *actor-side* E/M updates unchanged, but replace the critic by the *survival critic* induced by SDH (Sec. 4). Concretely, constraints affect learning *only* through critic targets via

$$\tilde{r}(s, a) = \alpha(s, a) r(s, a), \quad \tilde{\gamma}(s, a) = \gamma \alpha(s, a).$$

All KL budgets, dual updates, and policy-fitting details are exactly as in MPO.

What is different from original MPO? Relative to MPO, VT-MPO changes only:

1. the **score** used in the E-step (use Q_{surv} instead of the standard return critic), and
2. the **critic training target** (use shaped reward \tilde{r} and variable discount $\tilde{\gamma}$).

Everything else (E/M steps, KL constraints, trust region options, action sampling) is standard MPO.

F.1. Survival critic induced by SDH

Define the (unregularized) survival action-value function of a policy π as

$$Q_{\text{surv}}^\pi(s, a) := \mathbb{E}_{\tau \sim \pi} \left[\sum_{t \geq 0} u_t \tilde{r}(s_t, a_t) \mid s_0 = s, a_0 = a \right], \quad u_t := \prod_{k=0}^{t-1} \tilde{\gamma}(s_k, a_k), \quad (52)$$

which is the unique fixed point of the variable-discount Bellman recursion

$$Q_{\text{surv}}^\pi(s, a) = \tilde{r}(s, a) + \tilde{\gamma}(s, a) \mathbb{E}_{s' \sim P(\cdot | s, a)} \left[\mathbb{E}_{a' \sim \pi(\cdot | s')} [Q_{\text{surv}}^\pi(s', a')] \right]. \quad (53)$$

This is the critic used by VT-MPO.

F.2. Policy improvement (unchanged MPO E/M steps)

Fix an update state distribution d (estimated from replay) and a behavior/reference policy π_0 (typically the current actor, as in MPO). Given a critic estimate $Q_{\text{surv}}^{\pi_\theta}$, the nonparametric MPO improvement problem becomes

$$\max_q \mathbb{E}_{s \sim d} \left[\mathbb{E}_{a \sim q(\cdot | s)} Q_{\text{surv}}^{\pi_\theta}(s, a) \right] \quad \text{s.t.} \quad \mathbb{E}_{s \sim d} \left[\text{KL}(q(\cdot | s) \parallel \pi_0(\cdot | s)) \right] \leq \varepsilon, \quad (54)$$

(with $\int q(\cdot | s) da = 1$ for each s). The solution is the standard Boltzmann form

$$q^*(a | s) \propto \pi_0(a | s) \exp\left(\frac{1}{\eta} Q_{\text{surv}}^{\pi_\theta}(s, a)\right), \quad (55)$$

where the dual temperature $\eta > 0$ is chosen to satisfy the KL budget (exactly as in MPO). The M-step then fits the parametric actor to q^* using the same objective/parameterization as MPO (e.g. weighted maximum-likelihood or reverse KL), optionally with an additional trust region to the previous actor. *No actor-side changes are required beyond substituting Q_{surv} for the usual critic.*

F.3. Off-policy critic learning with variable discount

VT-MPO learns $Q_\phi \approx Q_{\text{surv}}^{\pi_\theta}$ off-policy using replay and a target network ϕ^- . The only modification to standard off-policy regression is that targets use $(\tilde{r}, \tilde{\gamma})$.

Virtual termination and done handling. Constraint events do *not* reset the simulator; “termination” is purely objective-level through $\alpha(s, a)$. Environment termination is handled normally via `done`: for true terminal transitions we disable bootstrapping by multiplying the bootstrap term by $(1 - \text{done})$. (Time-limit truncations may still bootstrap, using the standard timeout mask.)

Compressed TD(n) replay (engineering choice). To avoid storing full sequences for per-step corrections, we use a compressed n -step format that precomputes the survival-shaped return within the rollout window. For each time t , define

$$R_{t, \tilde{\gamma}}^{(n)} := \sum_{k=0}^{n-1} u_{t,k} \tilde{r}_{t+k}, \quad u_{t,k} := \prod_{j=0}^{k-1} \tilde{\gamma}_{t+j}, \quad u_{t,n} := \prod_{j=0}^{n-1} \tilde{\gamma}_{t+j}. \quad (56)$$

The replay buffer stores $(s_t, a_t, R_{t, \tilde{\gamma}}^{(n)}, s_{t+n}, u_{t,n}, \text{done}_{t+n})$. The TD(n) target is

$$y_t = R_{t, \tilde{\gamma}}^{(n)} + (1 - \text{done}_{t+n}) u_{t,n} \mathbb{E}_{a \sim \pi_\theta(\cdot | s_{t+n})} [Q_{\phi^-}(s_{t+n}, a)], \quad (57)$$

where the expectation is approximated by averaging $Q_{\phi^-}(s_{t+n}, a)$ over multiple action samples from the actor (as commonly done in MPO implementations).

Remark (off-policy corrections). Original MPO suggests sequence-based corrections (e.g. Retrace) for off-policy evaluation. Our compressed replay format does not retain the per-step information required for such corrections, so we do not apply them. Empirically, TD(n) with survival-shaped $(\tilde{r}, \tilde{\gamma})$ was stable in our settings (Sec. 6).

F.4. VT-MPO Summary

VT-MPO can be read as:

$$\text{VT-MPO} = \text{MPO (unchanged actor)} + \text{survival-shaped critic trained with } (\tilde{r}, \tilde{\gamma}).$$

Thus, constraints influence learning only through the critic targets, while replay-based off-policy policy improvement remains exactly MPO.

G. Absorbing State (Real Termination): Uniform Prior Structure, AS-SAC, and Dual Temperature Updates

This section unifies three consequences of the CaI+AS objective under a *normalized uniform* action prior: (i) the objective contains a feasibility-weighted *living cost* and therefore is not identical to standard MaxEnt-RL, (ii) AS admits a SAC-style off-policy solution because policy evaluation collapses to a single soft Bellman recursion under the survival-shaped dynamics, and (iii) learning the temperature κ is non-trivial under AS because constants are no longer ignorable; nevertheless, the objective admits a useful *two-critic decomposition* whose TD targets are independent of κ , enabling a stable off-policy dual update.

G.1. Exact CaI+AS objective under a normalized uniform prior

Recall Thm. C.1 (AS semantics):

$$\mathcal{J}_{\text{AS}}(\pi) = \mathbb{E}_{\tau \sim \pi} \left[\sum_{t \geq 0} \gamma^t \left(\prod_{k=0}^t \alpha_k \right) r_t - \kappa \sum_{t \geq 0} \gamma^t \left(\prod_{k=0}^{t-1} \alpha_k \right) \log \frac{\pi(a_t \mid s_t)}{\pi_0(a_t \mid s_t)} \right], \quad (58)$$

where $\alpha_k \equiv \alpha(s_k, a_k)$ and $r_t \equiv r(s_t, a_t)$.

Assume the prior is *uniform and normalized* so that its log-density is a global constant:

$$\log \pi_0(a \mid s) = -\ell_c \quad \forall (s, a). \quad (59)$$

(For $|\mathcal{A}| < \infty$, $\ell_c = \log |\mathcal{A}|$; in continuous control, ℓ_c corresponds to a chosen reference measure/volume and is typically implemented via a target-entropy constant.)

Define the AS survival-to-decision weight

$$w_t(\tau) := \gamma^t \prod_{k=0}^{t-1} \alpha(s_k, a_k), \quad (\text{empty product } \prod_{k=0}^{-1} \cdot \equiv 1), \quad (60)$$

and the survival-shaped reward/discount

$$\tilde{r}(s, a) := \alpha(s, a) r(s, a), \quad \tilde{\gamma}(s, a) := \gamma \alpha(s, a). \quad (61)$$

Corollary G.1 (CaI+AS with normalized uniform prior: entropy plus feasibility-weighted living cost). *Under (59), the exact objective (58) equals*

$$\mathcal{J}_{\text{AS}}(\pi) = \mathbb{E}_{\tau \sim \pi} \left[\sum_{t \geq 0} w_t(\tau) \left(\tilde{r}(s_t, a_t) + \kappa \mathcal{H}(\pi(\cdot \mid s_t)) - \kappa \ell_c \right) \right]. \quad (62)$$

Equivalently, writing the feasibility-weighted decision mass

$$Z(\pi) := \mathbb{E}_{\tau \sim \pi} \left[\sum_{t \geq 0} w_t(\tau) \right], \quad (63)$$

we can decompose

$$\mathcal{J}_{\text{AS}}(\pi) = \underbrace{\mathbb{E}_{\tau \sim \pi} \left[\sum_{t \geq 0} w_t(\tau) (\tilde{r}_t + \kappa \mathcal{H}(\pi(\cdot \mid s_t))) \right]}_{\text{"SAC-like" survival-shaped MaxEnt return}} - \underbrace{\kappa \ell_c Z(\pi)}_{\text{feasibility-weighted living cost}}. \quad (64)$$

In contrast to standard discounting (where $\sum_t \gamma^t$ is constant), $Z(\pi)$ depends on π through $\alpha(s, a)$, so the living-cost term is generally not an additive constant and cannot be dropped without changing the optimizer.

Remark G.2 (Finite action spaces and induced horizon regularization). If $|\mathcal{A}| < \infty$ and $\pi_0(a \mid s) = 1/|\mathcal{A}|$, then $\ell_c = \log |\mathcal{A}|$ and (64) contains the explicit feasibility-weighted living cost

$$\kappa \ell_c Z(\pi) = \kappa(\log |\mathcal{A}|) \mathbb{E}_{\tau \sim \pi} \left[\sum_{t \geq 0} \gamma^t \prod_{k=0}^{t-1} \alpha(s_k, a_k) \right].$$

Thus, under AS semantics, the normalized uniform prior imposes an *implicit regularization* on the expected feasibility-weighted decision horizon $Z(\pi)$: continuing to produce feasible decisions must be justified by sufficient feasible return (reward and/or entropy) to offset the constant per-decision cost.

Counter-Example G.3 (Stochastic optimum: dropping $-\kappa \ell_c Z(\pi)$ changes the optimizer). We give an MDP where the maximizer of \mathcal{J}_{AS} differs from that of $\mathcal{J}_{\text{AS-N}}$ (the objective with the $-\kappa \ell_c Z(\pi)$ term removed), *even though the optimal policies are strictly stochastic in both cases*.

MDP. Let $\mathcal{S} = \{s\}$ and $\mathcal{A} = \{a_{\text{cont}}, a_{\text{stop}}\}$ with $P(s \mid s, a) = 1$. Define $\alpha(s, a_{\text{cont}}) = 1$ and $\alpha(s, a_{\text{stop}}) = 0$, and rewards $r(s, a_{\text{cont}}) = r > 0$, $r(s, a_{\text{stop}}) = 0$. Assume the normalized uniform prior $\pi_0(a \mid s) = \frac{1}{2}$, hence $\ell_c = \log 2$.

Policy class. Consider stationary stochastic policies π_p with $\pi_p(a_{\text{cont}} \mid s) = p$, $\pi_p(a_{\text{stop}} \mid s) = 1 - p$, $p \in (0, 1)$, and let $h(p) := -p \log p - (1 - p) \log(1 - p)$ denote the binary entropy.

Compute the exact AS objective. In this MDP, survival-to-decision at time t requires choosing a_{cont} for all $k < t$, which occurs with probability p^t , so $\mathbb{E}[w_t(\tau)] = (\gamma p)^t$ and $\mathbb{E}[w_t(\tau) \alpha_t r_t] = (\gamma p)^t (pr)$. Since $\mathcal{H}(\pi_p(\cdot \mid s)) = h(p)$, (62) yields

$$\mathcal{J}_{\text{AS}}(\pi_p) = \sum_{t \geq 0} (\gamma p)^t (pr + \kappa h(p) - \kappa \log 2) = \frac{pr + \kappa h(p) - \kappa \log 2}{1 - \gamma p}.$$

Removing the living cost gives

$$\mathcal{J}_{\text{AS-N}}(\pi_p) = \frac{pr + \kappa h(p)}{1 - \gamma p}.$$

Different stochastic maximizers. Both objectives have interior maximizers (strictly stochastic optima) for $\kappa > 0$, but in general these maximizers differ because the constant $-\kappa \log 2$ is amplified by the effective horizon factor $\frac{1}{1 - \gamma p}$. For instance, with $(\gamma, \kappa, r) = (0.9, 1, 0.4)$,

$$\arg \max_{p \in (0, 1)} \mathcal{J}_{\text{AS}}(\pi_p) \approx 0.707, \quad \arg \max_{p \in (0, 1)} \mathcal{J}_{\text{AS-N}}(\pi_p) \approx 0.984.$$

G.2. AS implies a SAC-style soft Bellman recursion under survival shaping

Under AS, policy evaluation collapses to a single soft value function on the survival-shaped MDP with $(\tilde{r}, \tilde{\gamma})$ in (61). Concretely, for a fixed π and normalized uniform prior, the associated soft Bellman recursion can be written in the standard SAC form

$$Q^\pi(s, a) = \tilde{r}(s, a) - \kappa \ell_c + \tilde{\gamma}(s, a) \mathbb{E}_{s' \sim P(\cdot \mid s, a)} [V^\pi(s')], \quad V^\pi(s) := \mathbb{E}_{a \sim \pi(\cdot \mid s)} [Q^\pi(s, a) - \kappa \log \pi(a \mid s)]. \quad (65)$$

Because $\tilde{\gamma}(s, a) \leq \gamma < 1$, the corresponding Bellman operator remains a γ -contraction (Lem. C.6), hence admits stable off-policy TD learning with replay.

Equivalent “immediate KL” form (used by the two-critic split). An equivalent evaluation identity is obtained by defining $\bar{Q}^\pi(s, a) := Q^\pi(s, a) - \kappa \log \pi(a \mid s)$ and $\bar{V}^\pi(s) := \mathbb{E}_{a \sim \pi} [\bar{Q}^\pi(s, a)]$, which yields

$$\bar{Q}^\pi(s, a) = \tilde{r}(s, a) - \kappa (\log \pi(a \mid s) + \ell_c) + \tilde{\gamma}(s, a) \mathbb{E}_{s'} [\bar{V}^\pi(s')].$$

The two-critic decomposition in Sec. G.4 exploits precisely this “immediate KL” representation to learn the reward and KL components with TD targets that do not depend on κ .

AS-SAC critic target (single-critic view). For a replay transition $(s, a, r, s', d) \sim \mathcal{D}$, define $\alpha = \alpha(s, a)$, $\tilde{r} = \alpha r$, and $\tilde{\gamma} = (1 - d)\gamma\alpha$. Sampling $a' \sim \pi_\phi(\cdot | s')$, a SAC-style target consistent with (65) is

$$\hat{V}(s') := \min_{i \in \{1, 2\}} \bar{Q}_{\bar{\theta}_i}(s', a') - \kappa \log \pi_\phi(a' | s'), \quad y := \tilde{r} - \kappa \ell_c + \tilde{\gamma} \hat{V}(s'). \quad (66)$$

This differs from standard SAC only through survival shaping $(\tilde{r}, \tilde{\gamma})$ and the living-cost baseline $-\kappa \ell_c$.

Implementation note (continuous control). In continuous-action implementations, the normalized-uniform constant ℓ_c is instantiated via a chosen target-entropy baseline (cf. \mathcal{H}_{tgt} below). In ablations one may set this baseline to 0 (dropping the living cost), but counter-example G.3 shows this can change the optimizer under AS when α depends on the induced visitation.

G.3. What constraint does κ optimize under AS? (Why constants matter)

If κ is treated as fixed, no dual update is needed. If instead κ is adapted (SAC-style), then under AS a temperature dual should be derived against an AS-consistent notion of “per-step” entropy. In standard SAC, a temperature dual is often motivated by an *average* entropy constraint. Under AS with stochastic horizons, the natural notion of “per-step” is *per feasible decision*, weighted by w_t .

AS-consistent target entropy. A principled constraint is the *AS-weighted average entropy*

$$\frac{1}{Z(\pi)} \mathbb{E}_{\tau \sim \pi} \left[\sum_{t \geq 0} w_t(\tau) \mathcal{H}(\pi(\cdot | s_t)) \right] \geq \bar{\mathcal{H}}, \quad (67)$$

with $Z(\pi)$ from (63). A corresponding (un-normalized) Lagrangian dual loss is

$$\mathcal{L}_\kappa^{\text{AS}}(\kappa) := \mathbb{E}_{\tau \sim \pi} \left[\sum_{t \geq 0} w_t(\tau) \kappa (-\log \pi(a_t | s_t) - \bar{\mathcal{H}}) \right]. \quad (68)$$

Key insight: unlike standard SAC, the constant term $-\kappa \bar{\mathcal{H}} Z(\pi)$ is *policy dependent* because $Z(\pi)$ is policy dependent; dropping it generally changes the optimizer (cf. counter-example G.3).

Equivalent KL-to-uniform view. Under the normalized uniform prior, for each state s ,

$$D_{\text{KL}}(\pi(\cdot | s) \| \pi_0(\cdot | s)) = -\mathcal{H}(\pi(\cdot | s)) + \ell_c. \quad (69)$$

Thus an AS-weighted KL budget is equivalent to (67) with $\bar{\mathcal{H}} = \ell_c - \bar{\ell}$.

G.4. Two-critic decomposition (targets independent of κ)

The AS objective with a uniform prior has additional structure that is especially useful when κ is learned: it can be written as the value of a difference of two $\tilde{\gamma}$ -discounted critics whose TD targets do not contain κ . This trick is used in Algorithm 3.

Define two $\tilde{\gamma}$ -discounted critics. Fix π and define

$$\tilde{Q}_R^\pi(s, a) := \mathbb{E}_\pi \left[\sum_{t \geq 0} \left(\prod_{k=0}^{t-1} \tilde{\gamma}(s_k, a_k) \right) \tilde{r}(s_t, a_t) \mid s_0 = s, a_0 = a \right], \quad (70)$$

$$Q_{\text{KL}}^\pi(s, a) := \mathbb{E}_\pi \left[\sum_{t \geq 0} \left(\prod_{k=0}^{t-1} \tilde{\gamma}(s_k, a_k) \right) (\log \pi(a_t | s_t) + \mathcal{H}_{\text{tgt}}) \mid s_0 = s, a_0 = a \right], \quad (71)$$

where \mathcal{H}_{tgt} is a constant; for the exact uniform-prior objective, set

$$\mathcal{H}_{\text{tgt}} = \ell_c. \quad (72)$$

Both critics satisfy standard Bellman equations under $(\tilde{r}, \tilde{\gamma})$:

$$\tilde{Q}_R^\pi(s, a) = \tilde{r}(s, a) + \tilde{\gamma}(s, a) \mathbb{E}_{s' \sim P(\cdot | s, a)} [V_R^\pi(s')], \quad (73)$$

$$Q_{\text{KL}}^\pi(s, a) = (\log \pi(a | s) + \mathcal{H}_{\text{tgt}}) + \tilde{\gamma}(s, a) \mathbb{E}_{s' \sim P(\cdot | s, a)} [V_{\text{KL}}^\pi(s')], \quad (74)$$

with $V_R^\pi(s) = \mathbb{E}_{a \sim \pi} [\tilde{Q}_R^\pi(s, a)]$ and $V_{\text{KL}}^\pi(s) = \mathbb{E}_{a \sim \pi} [Q_{\text{KL}}^\pi(s, a)]$.

Combined value and exact actor objective. Define

$$Q_\kappa^\pi(s, a) := \tilde{Q}_R^\pi(s, a) - \kappa Q_{\text{KL}}^\pi(s, a), \quad V_\kappa^\pi(s) := \mathbb{E}_{a \sim \pi(\cdot|s)}[Q_\kappa^\pi(s, a)]. \quad (75)$$

Proposition G.4 (Exact value representation and actor objective). *t* Fix a policy π and set $\mathcal{H}_{\text{tgt}} = \ell_c$ in (71). Let Q_κ^π and V_κ^π be defined as in (75). Then the CaI+AS objective under a normalized uniform prior satisfies

$$\mathcal{J}_{\text{AS}}(\pi) = \mathbb{E}_{s_0 \sim p(s_0)}[V_\kappa^\pi(s_0)]. \quad (76)$$

Consequently, any policy improvement step consistent with \mathcal{J}_{AS} may maximize

$$\mathbb{E}_{s \sim d} \mathbb{E}_{a \sim \pi(\cdot|s)} \left[\tilde{Q}_R^\pi(s, a) - \kappa Q_{\text{KL}}^\pi(s, a) \right] = \mathbb{E}_{s \sim d} \mathbb{E}_{a \sim \pi(\cdot|s)} [Q_\kappa^\pi(s, a)], \quad (77)$$

for any chosen state distribution d (e.g. replay). In off-policy learning, replacing the true critics by learned approximations yields the equivalent minimization loss

$$\mathcal{L}_\pi(\phi) = \mathbb{E}_{s \sim \mathcal{D}} \mathbb{E}_{a \sim \pi_\phi(\cdot|s)} \left[\kappa \hat{Q}_{\text{KL}}(s, a) - \hat{Q}_R(s, a) \right]. \quad (78)$$

Remark G.5 (No extra $\kappa \log \pi$ term (avoid double counting)). By definition, Q_{KL}^π in (71) already includes the *current-step* information term $\log \pi(a | s)$ (and the baseline \mathcal{H}_{tgt}). Therefore, the actor loss (78) already accounts for the immediate entropy/KL contribution through $\kappa \hat{Q}_{\text{KL}}(s, a)$. Naïvely adding an additional $\kappa \log \pi_\phi(a | s)$ term would generally *double count* this contribution at the level of the *objective value* and thus optimize a different objective.

Proof of Prop. G.4. Subtract κ times the Bellman recursion (74) from (73) to obtain, for all (s, a) ,

$$Q_\kappa^\pi(s, a) = \tilde{r}(s, a) - \kappa(\log \pi(a | s) + \mathcal{H}_{\text{tgt}}) + \tilde{\gamma}(s, a) \mathbb{E}_{s' \sim P(\cdot|s, a)} [V_\kappa^\pi(s')]. \quad (79)$$

Unrolling (79) along a trajectory generated by π yields

$$V_\kappa^\pi(s_0) = \mathbb{E}_{\tau \sim \pi} \left[\sum_{t \geq 0} \left(\prod_{k=0}^{t-1} \tilde{\gamma}_k \right) \left(\tilde{r}_t - \kappa(\log \pi(a_t | s_t) + \mathcal{H}_{\text{tgt}}) \right) \middle| s_0 \right], \quad (80)$$

where $\tilde{r}_t = \tilde{r}(s_t, a_t)$ and $\tilde{\gamma}_k = \tilde{\gamma}(s_k, a_k)$. Now set $\mathcal{H}_{\text{tgt}} = \ell_c$ and use $\prod_{k=0}^{t-1} \tilde{\gamma}_k = \gamma^t \prod_{k=0}^{t-1} \alpha_k = w_t(\tau)$ and $\tilde{r}_t = \alpha_t r_t$ to rewrite (80) as

$$V_\kappa^\pi(s_0) = \mathbb{E}_{\tau \sim \pi} \left[\sum_{t \geq 0} w_t(\tau) \left(\alpha_t r_t - \kappa(\log \pi(a_t | s_t) + \ell_c) \right) \middle| s_0 \right],$$

which matches the uniform-prior CaI+AS objective conditioned on s_0 (cf. (62)). Averaging over $s_0 \sim p(s_0)$ gives (76).

Finally, since $Q_\kappa^\pi = \tilde{Q}_R^\pi - \kappa Q_{\text{KL}}^\pi$ and $V_\kappa^\pi(s) = \mathbb{E}_{a \sim \pi(\cdot|s)}[Q_\kappa^\pi(s, a)]$, a policy improvement step can maximize the state-averaged value $\mathbb{E}_{s \sim d} \mathbb{E}_{a \sim \pi}[Q_\kappa^\pi(s, a)]$, yielding (77). Replacing expectations under d by replay sampling and Q -functions by learned critics gives the actor loss (78). \square

Gradient-improved actor loss (optional; same value, SAC-style entropy gradient). While the objective value in (78) should not be modified by appending an extra $\kappa \log \pi_\phi(a | s)$ term (Remark G.5), it can be useful in practice to expose an *explicit* SAC-style entropy gradient path. This issue arises because in off-policy implementations Q_{KL} is typically trained with a stabilized TD target that treats the current-step log-probability as a constant, e.g. via $\text{sg}[\log \pi_\phi(a | s)]$ in (85). As a result, when \hat{Q}_{KL} is used inside the actor loss, the policy gradient may rely predominantly on the action-through-critic path and can be more sensitive to critic noise.

A standard remedy is to add and subtract the same quantity, where the subtracted copy is stop-gradient, so that the *scalar objective value* is unchanged but the *actor gradient* gains the desired entropy term. Define the per-decision information cost

$$c_{\text{KL}}(s, a) := \log \pi_\phi(a | s) + \mathcal{H}_{\text{tgt}}, \quad (81)$$

and consider

$$\mathcal{L}_\pi^{\text{GI}}(\phi) = \mathbb{E}_{s \sim \mathcal{D}, a \sim \pi_\phi(\cdot | s)} \left[\kappa \hat{Q}_{\text{KL}}(s, a) - \hat{Q}_R(s, a) + \kappa(c_{\text{KL}}(s, a) - \text{sg}[c_{\text{KL}}(s, a)]) \right]. \quad (82)$$

Since $\text{sg}[c_{\text{KL}}] = c_{\text{KL}}$ as a *value*, the expectation in (82) equals that of (78); thus both losses represent the same objective value and (under exact critics) share the same maximizers. However, the added difference term has zero value but contributes $\nabla_\phi c_{\text{KL}} = \nabla_\phi \log \pi_\phi(a | s)$ to the actor update, yielding an explicit SAC-style entropy/KL gradient *without* double counting in the objective value.

G.5. Off-policy TD targets and a practical dual update for κ

Critic TD targets (independent of κ). For a replay transition $(s, a, r, s', d) \sim \mathcal{D}$, set

$$\alpha := \alpha(s, a), \quad \tilde{\gamma} := (1 - d)\gamma\alpha. \quad (83)$$

Sample $a' \sim \pi_\phi(\cdot | s')$. Using double critics and target networks, define

$$y_R := \alpha r + \tilde{\gamma} \min_{i \in \{1, 2\}} \bar{Q}_{R, \bar{\theta}_i}(s', a'), \quad (84)$$

$$y_{\text{KL}} := (\text{sg}[\log \pi_\phi(a | s)] + \mathcal{H}_{\text{tgt}}) + \tilde{\gamma} \min_{i \in \{1, 2\}} \bar{Q}_{\text{KL}, \bar{\psi}_i}(s', a'). \quad (85)$$

Both critics are trained with standard MSE regression:

$$\mathcal{L}_R(\theta_i) = \mathbb{E}[(Q_{R, \theta_i}(s, a) - y_R)^2], \quad \mathcal{L}_{\text{KL}}(\psi_i) = \mathbb{E}[(Q_{\text{KL}, \psi_i}(s, a) - y_{\text{KL}})^2]. \quad (86)$$

Dual update for κ via a discounted KL-mass budget. While (68) is the AS-consistent entropy constraint, implementing it literally requires trajectory-level weights and (optionally) normalization by $Z(\pi)$. The two-critic decomposition provides a simpler off-policy alternative: constrain the *AS-discounted total KL mass* estimated by Q_{KL} ,

$$\mathbb{E}_{s \sim \mathcal{D}, a \sim \pi_\phi(\cdot | s)} [\hat{Q}_{\text{KL}}(s, a)] \leq \varepsilon. \quad (87)$$

Parameterize $\kappa = \exp(\eta)$ for positivity. A stable dual loss is

$$\mathcal{L}_\kappa(\eta) = -\exp(\eta) \left(\mathbb{E}_{s \sim \mathcal{D}, a \sim \pi_\phi} [\hat{Q}_{\text{KL}}(s, a)] - \varepsilon \right). \quad (88)$$

Setting $\varepsilon = 0$ and $\mathcal{H}_{\text{tgt}} = \ell_c$ encourages the policy toward the uniform prior in the AS-discounted sense. (Enforcing a normalized ‘‘per-decision average’’ would additionally require estimating $Z(\pi)$, e.g. with an extra Q_Z critic; we do not pursue this here.)

G.6. Algorithm summary (Two-Critic AS-SAC)

At each gradient step:

1. Sample $(s, a, r, s', d) \sim \mathcal{D}$.
2. Compute $\alpha = \alpha(s, a)$, $\tilde{r} = \alpha r$, $\tilde{\gamma} = (1 - d)\gamma\alpha$.
3. Sample $a' \sim \pi_\phi(\cdot | s')$ and form y_R, y_{KL} via (84)–(85).
4. Update (Q_R, Q_{KL}) by minimizing (86).
5. Update actor by minimizing (78) (or (82)).
6. Update temperature by minimizing (88).

This reduces to standard SAC when $\alpha \equiv 1$ (so $\tilde{\gamma} \equiv \gamma$ and $Z(\pi)$ is constant), while for general $\alpha(s, a)$ it remains replay-compatible and correctly accounts for the AS-specific living-cost structure.